Development of Plasma-based DNA Methylation Markers for the Detection of Hepatocellular Carcinoma

KAN, Hoi Lam

A Thesis Submitted in Partial Fulfilment

of the Requirements for the Degree of

Master of Philosophy

in

Chemical Pathology

The Chinese University of Hong Kong

August 2009

ABSTRACT

Development of Plasma-based DNA Methylation Markers for the Detection of Hepatocellular Carcinoma

Submitted by KAN Hoi Lam for thesis submitted for the degree of Master of Philosophy in Chemical Pathology at The Chinese University of Hong Kong in June 2009

Hepatocellular carcinoma (HCC) is the fifth most common cancers in the world and is the third leading cause of cancer death (Parkin *et al*, 2005). The diagnosis of HCC relies on the measurement of serum α-fetoprotein (AFP) level which has already been used for 40 years. The discovery of promoter hypermethylation of tumor suppressor genes (TSGs) in HCC tissues has opened up the possibility of using methylated TSGs as potential markers for HCC.

Methylation-specific PCR (MSP) has been a commonly used technique for the detection of aberrant DNA methylation. However, the detection rates of methylated TSGs in blood using MSP were much lower that their detection in tumor tissues. This was likely resulted from the degradation of DNA during the bisulfite conversion step of MSP (Grunau *et al*, 2001). In this regard, Chan *et al.* developed a non-bisulfite-based approach to detect methylated *RASSF1A* in plasma (Chan *et al*, 2008a). This method is termed methylation-sensitive restriction enzymes-mediated real-time quantitative PCR (MSRE-qPCR). Using this method, hypermethylated *RASSF1A* sequences could be detected in the serum of 93% HCC patients (Chan *et al*, 2008a). As the sensitivity was remarkably enhanced by this approach, low concentrations of methylated *RASSF1A* sequences

were also detected in the serum of 58% hepatitis B virus (HBV) carriers. This observation was postulated to be due to the release of methylated sequences from the nonmalignant hepatitic liver as the hypermethylation of *RASSF1A* is an early event in HCC pathogenesis and could be observed in patients with nonmalignant conditions such as cirrhosis and chronic hepatitis (Chan *et al*, 2008a). In this project, I have studied the detectability of other aberrantly methylated TSGs in the plasma of HCC patients to determine if the combination of these markers can provide a more accurate diagnostic test for HCC than using *RASSF1A* alone.

Using MSRE-qPCR, promotor hypermethylation of *GSTP1*, *SOCS1*, *APC* and *p16* genes was detected in the tumor tissues of 78.6%, 64.3%, 87.5% and 89.3% HCC patients (n=55), respectively. The detection rates for these aberrantly methylated sequences in the plasma samples of HCC patients were 42.9%, 35.7%, 32.1% and 58.9%, respectively. In contrast, these sequences were respectively detected in 3.6%, 3.6%, 0% and 9.1% of chronic hepatitis B carriers (n=56). Aberrantly methylated *GSTP1*, *SOCS1* and *p16* sequences were not detectable in any of the healthy control subjects (n=58) whereas methylated *APC* sequences were detected in 3.4% healthy subjects. Overall, 76.8%, 14.5% and 3.4% of HCC patients, HBV carriers and healthy subjects, respectively, had one or more aberrantly methylated tumor suppressor genes (*GSTP1* / *SOCS1* / *APC* / *p16*) detected in plasma. In addition, 72.0% HCC patients with normal serum AFP concentration had at least one aberrantly methylated tumor suppressor gene detected in plasma. The combination of plasma methylation markers with AFP measurement increased the sensitivity of HCC detection from 55.4% to 87.5% while the specificity is decreased from 90.9% to 78.2%.

In conclusion, the detection of aberrantly methylated *GSTP1*, *SOCS1*, *APC* and *p16* genes in plasma using MSRE-qPCR is potentially useful for the detection of HCC. In contrast to *RASSF1A*, aberrantly methylated sequences of these four TSGs are infrequently detected in the plasma of chronic HBV carriers. These tests can also be used in conjunction with AFP measurement to achieve better diagnostic accuracy.

摘要

肝細胞癌(HCC)是全球第 5 位常見的惡性腫瘤，在全球癌症死亡率中居第三位。近 40 年來，衡量血清甲胎蛋白(AFP)的水準是診斷肝細胞癌的主要手段。研究發現肝細胞癌組織樣本中抑癌基因啓動子區域呈現高甲基化狀態，這一特點有望爲肝細胞癌的診斷提供新的標誌物。

甲基化特異性聚合酶鏈式反應 (Methylation-specific PCR, MSP)被廣泛應用於異常 DNA 甲基化的檢測，然而這一方法在血液樣本中對抑癌基因甲基化的檢出率遠遠低於腫瘤樣本。導致這一現象的原因可能是 MSP 之前的亞硫酸氫鹽修飾步驟中 DNA 降解。因此，Chan 等人開發了甲基化敏感限制酶切介導的即時定量 PCR (Methylation-sensitive restriction enzyme-mediated real-time quantitative PCR, MSRE-qPCR)，用於檢測血漿中的高甲基化的 *RASSF1A**基因，這一方法擺脫了亞硫酸氫鹽修飾的限制。利用這個方法，高甲基化的 *RASSF1A* 序列在肝細胞癌病人的血清中的檢出率達到了 93%。由於該方法具有很高的靈敏度，即使是在乙型肝炎帶菌者的血清中，對低濃度的高甲基化的 *RASSF1A* 序列的檢出率也達到了 58%。由於 *RASSF1A* 的高甲基化是肝細胞癌發病過程中的早期事件，並且在非惡性疾病，比如肝硬化和慢性肝炎的病人中，也觀察到這一現象。因此，我們推測血清中的高甲基化 *RASSF1A* 序列可能源自非惡性肝臟組織。在論文中，我嘗試在肝細胞癌病人的血漿中檢測多個抑癌基因的異常甲基化序列，以期檢定多個標誌物同時使用能否比單獨使用 *RASSF1A* 提高對肝細胞癌的診斷精確度。

利用 MSRE-qPCR，*GSTP1*, *SOCS1*, *APC*, *p16*$^{\#}$ 等基因的啓動子區域高甲基化在肝細胞癌病人的腫瘤樣本中的檢出率分別爲 78.6%, 64.3%, 87.5% 和

89.3%。這些高甲基化序列在肝細胞癌病人的血漿樣本中的檢出率分別爲 42.9%, 35.7%, 32.1% 和 58.9%。而在慢性乙型肝炎病人中這些序列的檢出率爲 3.6%, 3.6%, 0% 和 9.1%。在正常健康對照組中，所有樣本均檢測不到高甲基化的 *GSTP1, SOCS1* 和 *p16* 序列，其中 3.4%的樣本檢測到高甲基化的 *APC* 序列。總體上說，76.8%的肝細胞癌病人，14.5%的慢性乙型肝炎患者和 3.4%的健康對照組，可在血漿中檢測到一個或多個高甲基化序列 (*GSTP1* / *SOCS1* / *APC* / *p16*)。此外，在那些具有正常血清甲胎蛋白濃度的肝細胞癌病人中，72%的病人可在其血漿中檢測到至少一個高甲基化序列。如果將血漿中的高甲基化標誌物和血清中的甲胎蛋白檢測將結合，肝細胞癌的檢測靈敏度可以從 55.4% 提高至 87.5%，而其特異性則從 90.9% 輕微跌至 78.2%。

總括來說，利用 MSRE-qPCR 的方法在病人血漿中對 *GSTP1, SOCS1, APC* 和 *p16* 的高甲基化序列進行檢測，有助於診斷病人是否患有肝細胞癌。和 *RASSF1A* 不同的是，這四個基因的異常高甲基化序列在慢性乙型肝炎帶菌者中的檢出率並不高。這種方法和甲胎蛋白濃度檢測相結合能夠改善肝細胞癌的診斷精確度。

註釋：

**RASSF1A*: Ras 相關家族 1A 基因
#GSTP1: 穀胱苷肽 S 轉移酶 P1 基因
SOCS1: 細胞因數信號抑制因數-1 基因
APC: 結腸腺瘤性息肉病基因
p16: 週期蛋白依賴激酶抑制因數 2A 基因

ACKNOWLEDGEMENTS

I would like to express my gratitude to my supervisor Prof. Y. M. Dennis Lo for giving me the opportunity to join his team to further pursue studies in significant medical research. Under his supervision and guidance, I was inspired by his passion, work attitude and problem-solving process. The experience of working in this group was really invaluable and the skills learnt here were transferrable to any working environments.

My thanks must also go to Prof. Allen Chan, who provided me technical support in this project. From him, I have not only learnt research-related knowledge and skills, but also critical thinking and presentation skills. He did provide emotional care and support to me when I was depressed or frustrated. I would also like to thank Prof. Paul Lai of the Department of Surgery and Prof. Henry Chan of the Department of Medicine and Therapeutics for arranging sample collection.

Special thanks also go to every member of Prof. Lo's team for their love and care. I would like to thank Ms. Sze Wan Yeung for her patience, guidance and teaching. I would also like to thank Dr. Grace Tong for her advice and constructive discussion.

I wish to thank my parents to allow me to pursue further studies although in a financial hard time. I am thankful to their trust, support and care throughout the study period. I would also like to thank brothers and sisters in church for their

endless support and prayers.

Finally, my immense gratitude towards God cannot be expressed by words, for His everlasting love and precious salvation. I am also thankful for His ceaseless grace and strength given to me throughout the study period.

TABLE OF CONTENTS

LIST OF TABLES

LIST OF FIGURES

LIST OF ABBREVIATIONS

ACTB	*β-actin*
AFP	α-fetoprotein
AFU	α-L-fucosidase
APC	*Adenomatosis polyposis coli*
bp	Base pair
BRCA1	*Breast-cancer suspectibility gene 1*
CCD	Charge-coupled device
CIMP	CpG island methylator phenotype
COBRA	Combined bisulfite restriction analysis
C_T	Threshold cycle
DCP	Des-gamma-carboxy prothrombin
DMD	Differentially methylated domain
DNA	Deoxyribonucleic acid
DNMTs	DNA methyltransferases
dNTP	Deoxyribonucleotide triphosphate
EDTA	Ethylenediaminetetraacetic acid
ELISA	Enzyme-linked immunosorbent assay
FAM	6-carboxyfluorescein
FRET	Fluorescence resonance energy transfer
GP73	Golgi protein 73
GPC-3	Glypican-3
GSTP1	*Glutathione-S-transferase-Pi*
HBV	Hepatitis B virus
HCC	Hepatocellular carcinoma
HCV	Hepatitis C virus
HR	Hazard ratio
hTERT	Human telomerase reverse transcriptase
ICR	Imprinting control region
IGF-II	Insulin-like growth factor-II
IPTG	Isopropyl β-D-1-thiogalactopyranoside
JAK	Janus kinase
LCA	*Lens culinaris* agglutin
LEF-TCF	Lymphoid enhancer factor-T cell factor
MBPs	Methyl-CpG-binding proteins
$MgCl_2$	Magnesium chloride

µl	Microliter
MSP	Methylation-specific PCR
MSRE-qPCR	Methylation-sensitive restriction enzyme-mediated real-time quantitative PCR
Ms-SNuPe	Methylation sensitive single nucleotide primer extension
NFQ	Non-fluorogenic quencher
p16	*Cyclin-dependent kinase inhibitor 2A*
PCR	Polymerase chain reaction
qPCR	quantitative polymerase chain reaction
RASSF1A	*Ras association (RalGDS/AF-6) domain family member 1 isoform A*
RLGS	Restriction landmark genomic scanning
ROX	6-carboxy-x-rhodamine
SOC	Super optimal broth with catabolite repression
SOCS1	*Suppressor of cytokine signaling 1*
STAT	Signal transducer and activators of signalling pathways
TAMRA	6-carboxytetramethylrhodamine
Taq	*Thermus aquaticus*
TGF-β1	Transforming growth factor-β1
TSG	Tumor suppressor gene
X-Gal	bromo-chloro-indolyl-galactopyranoside
XIST	*X-(inactive)-specific transcript*

PUBLICATION

Conference abstract

Kan K.H.L., Chan K.C.A., Lai P.B.S., Chan H.L.Y., Yeung S.W. and Lo Y.M.D. Detecting hepatocellular carcinoma by analysis of aberrantly methylated promoter of *GSTP1* and *SOCS1* in plasma DNA using methylation-sensitive restriction endonucleases quantitative PCR. *Infection and Cancer: Biology, Therapeutics, and Prevention*, American Association for Cancer Research, Hong Kong, Dec 2008.

SECTION I: BACKGROUND

Chapter 1: Hepatocellular Carcinoma (HCC)

Hepatocellular carcinoma (HCC) is the fifth most common cancer in the world and is the third leading cause of cancer deaths (Parkin *et al*, 2005). The number of deaths associated with HCC remains high despite medical advances over the past few decades. HCC demonstrates a preferential geographic distribution in Sub-Saharan Africa and Asia where hepatitis B and C viral infections are prevalent (Bosch *et al*, 2004; Llovet *et al*, 2003). This fact has highlighted the importance of chronic viral infection as an etiology of HCC.

One important reason for the high mortality for HCC is the late presentation of the HCC patients as early HCC is typically asymptomatic. Over the last few decades, efforts have been paid to develop better diagnostic tools for detecting early HCC, particularly in high risk groups. However, the existing tests have failed to provide desirable sensitivity and specificity for HCC surveillance purpose.

This chapter will discuss the epidemiology, etiology and clinical presentation of HCC as well as the current diagnostic methods and treatment modalities for HCC patients, and also the past efforts in HCC marker development.

1.1. Epidemiology of HCC

In 2007, there were 711,000 new liver cancer cases and about 680,000 people died from liver cancer globally (Global Cancer Facts and Figures, American Cancer Society, 2007). HCC consists of 70-80% of total cases of liver cancer and this thesis would focus on it. HCC is the third cancer killer in men and the sixth in women. The male:female ratio for HCC is 3:1.

HCC demonstrates an unbalanced geographical distribution in which more than 80% of cases come from developing countries (Parkin *et al*, 2005). Areas with high HCC incidence in the past such as Hong Kong, Shanghai and Singapore, have shown a decrease in incidence while the HCC incidence in Central Europe and North America where HCC was rare in the past has increased. The reduction of HCC incidence in the former regions is thought to be attributed to the HBV vaccination programs and the better control of aflatoxin exposure in these areas. The increasing incidence in the latter regions may be due to the increasing prevalence of hepatitis C infection and the influx of immigrants from countries with high incidence (But *et al*, 2008; El-Serag *et al*, 2003).

1.2. Etiology of HCC

The pathogenesis of HCC is complex and involves the interactions of genetic

abnormalities, exposure to dietary and environmental hepatotoxins and infection with hepatotropic viruses. To date, the most established etiological factors for HCC include cirrhosis, HBV and HCV infections, and plant carcinogen aflatoxin B exposure.

1.2.1. Cirrhosis

About 80-90% of HCC patients were found to be associated with cirrhosis but cirrhosis does not always lead to HCC development (Llovet *et al*, 2003). Precancerous cirrhotic livers appear to have large nodules and thin intervening stroma which undergo vigorous regenerative activities and DNA synthesis. This cell regeneration process is an oncogenic event which promotes cell division, selection and clonal expansion of cells with malignant potential. Cirrhotic livers with adenomatosis hyperplastic nodules are considered as having high potential for HCC development (Borzio *et al*, 1995; Livraghi *et al*, 1997; Okuda, 1992). Three to five percent of cirrhotic patients would develop HCC each year (Sangiovanni *et al*, 2004; Tsukuma *et al*, 1993).

1.2.2. Hepatitis virus

HBV infection is an important risk factor for HCC especially if one acquires the infection early in life. HBV is highly endemic in Asia and sub-Saharan Africa. In this area, a lot of people contract HBV infection during childhood when their immunity against HBV is weak. As a result, they become chronic carriers of HBV. The risk for HCC development in chronic HBV carriers greatly depends on the age of acquiring

the infection. The lifetime risk is about 40% if infected in childhood and 10% if infected in adulthood. Overall, 0.26% to 0.6% of chronic HBV carriers would develop HCC each year. The risk would increase to 1% and 2-3% in patients with active hepatitis and cirrhosis, respectively (Michielsen *et al*, 2005). HBV infection can predispose to HCC possibly through viral integration into the host genome of the liver cells and result in transactivation of proto-oncogenes, inactivation of tumor suppressor genes, and activation of growth factors. The HBV encoded *HBx* gene can also act on cyclin A, protein kinases and DNA repair system and lead to HCC development (Chan & Sung, 2006).

Hepatitis C virus (HCV) infection is an important etiological factor for HCC in Japan and western countries. HCV-related HCC represents 70% of all cases in Japan (Umemura *et al*, 2009). In the U.S., 47% of HCC patients have been infected with HCV but only 15% of them have chronic HBV infection. HCV transmission is mainly through intravenous drug injection in drug abusers and transfusion of unscreened blood and blood products (El-Serag, 2004). The pathogenic mechanism involved in HCV-related HCC is likely to exhibit differences from that of HBV-associated HCC as HCV is a single-stranded RNA virus and is incapable of integrating into the genome of infected liver cell. HCV-related HCC is caused by chronic inflammation, cell death, proliferation and cirrhosis (But *et al*, 2008).

1.2.3. Plant carcinogens

Aflatoxin intake is a risk factor for HCC in developing areas of the subtropical regions of the world where the hygiene conditions and weather favor the growth of

the fungus *Aspergillus flavis*. People consume grains, peanuts and food products contaminated by aflatoxins are prone to develop HCC (Smela *et al*, 2001).

1.2.4. Miscellaneous factors

Alcohol consumption may not have direct carcinogenic effect on the liver. However, excessive consumption of alcohol can led to cirrhosis and hence, increase the risk of HCC development (Morgan *et al*, 2004). Potential carcinogens have also been identified in pharmaceutical, cosmetic products, cleaning reagents, organic solvents and pesticides (Lau, 2008).

1.3. Clinical presentation of HCC

HCC is usually asymptomatic until the tumor grows to a substantial size and invades the neighboring tissues. When a large proportion of the parenchyma is replaced by tumor cells and the rest of the liver reserves cannot sustain its functions, the clinical symptoms related to functional disturbances would start to appear (Lau, 2008). The symptoms of HCC are highly variable and include jaundice, ascites, palpable mass in the abdomen, pain, fever, variceal bleeding, anorexia, confusion and other constitutional syndrome (Livraghi *et al*, 1997). In patients presenting with symptoms of cirrhosis, they may die from liver failure instead of tumor invasion.

1.4. Existing diagnostic tests for HCC

1.4.1. Alpha-fetoprotein (AFP)

Serum alpha-fetoprotein (AFP) is the most commonly used tumor marker for HCC although it was first discovered forty years ago. AFP is a serum protein synthesized physiologically by fetal livers and its level would decline gradually after birth. However, AFP would also be secreted abnormally by HCC cells. A serum concentration of 20 μg/L is commonly used as a cut-off value to differentiate HCC patients from normal individuals. The diagnostic sensitivity of AFP for HCC is 40-60% and the specificity is 80-90% (Farinati *et al*, 2006; Wright *et al*, 2007). In addition, chronic hepatitis and cirrhotic patients may also have elevated AFP levels and this fact may limit the application of AFP measurement for detecting HCC in this group of patients (Zhou *et al*, 2006). In this regard, a search of better markers that are more sensitive and specific for HCC is an ongoing effort by workers in the field (Marrero & Lok, 2004).

1.4.2. Imaging

Ultrasound is a common imaging modality that is used complementarily with AFP measurement for the screening of HCC. It is relatively inexpensive, safe and easy to perform. However, it is operator-dependent and labor-intensive. As a large proportion of HCC patients have cirrhotic livers, accurate differentiation between small HCC and benign liver lesions may be difficult (Rapaccini *et al*, 2004). Computer-assisted tomography is also a commonly utilized imaging technique for HCC detection. It is particularly useful for measuring the size of the tumor, detecting metastasis and identifying vascular invasion.

1.5. Treatment of HCC

Tumor resection and liver transplantation are the two common treatment modalities that can be used with curative intent. Palliative treatments like tumor ablation or embolization are also offered to patients that are not curable with surgery for symptomatic relief.

1.5.1. Surgical Resection and Transplantation

The median 5-year survival rates for patients who have undergone surgical resection and transplantation are approximately 50% and 70%, respectively (Llovet *et al*, 1999). However, less than one third of HCC patients are suitable for surgical resection of the tumor as most patients present with either locally advanced diseases or distant metastases. Moreover, many HCC patients have cirrhosis and the regenerating capacity of the hepatocytes is greatly compromised. In such patients, as the portion of resectable liver is limited and the residual liver tissue may be prone to exhibit tumor recurrence. In this regard, liver transplantation may be used for patients with cirrhosis and poor liver function reserves. However, the limiting factor for liver transplantation is always the difficulty in having organ donation opportunities.

1.5.2. Tumor Ablation or Embolization

For patients not suitable for curative-intent tumor resection, tumor ablation or

embolization methods can be used as palliative treatments. Ablation refers to local methods of tumor destruction and includes radiofrequency ablation, cryosurgery and ethanol injection. Radiofrequency ablation uses a needle-like probe to release high frequency alternating current and produces frictional heating to destroy tumor cells. Cryosurgery uses a very cold metal probe to freeze and destroy tumor cells. Ethanol injection destroys the tumor by injecting concentrated alcohol directly into the tumor to kill cancer cells.

Embolization involves the blockage of a blood-supplying artery to the tumor by surgical or chemical means (chemoembolization). The principle is to delay the invasion and progression of the cancer by depriving the tumor of nutrient supplies. However, embolization of arteries also reduces blood supply for normal liver tissues. Studies in the Caucasians and Japanese showed that chemoembolization is effective and results in 5-year survival rates higher than 50% in patients who have received this treatment (Llovet & Bruix, 2003).

1.5.3. Chemotherapy and Radiotherapy

Doxorubicin is the most effective chemotherapeutic agent that shrinks the size of the tumor. Doxorubicin is a topoisomerase II inhibitor and it suppresses tumor growth by inhibiting DNA synthesis and interfering with DNA strand separation and helicase activity (Gewirtz, 1999). The drug can be administered intravenously or orally. However, chemotherapeutic drugs often produce side effects as it also kills some normal cells. Side effects include nausea, vomiting, loss of appetite, loss of hair, and mouth sores. More severe side effects also include susceptibility to infection,

bleeding tendency and anemia because of bone marrow suppression.

Radiation therapy can shrink the tumor and alleviate symptoms like pain although it does not improve survival of HCC. With advanced imaging techniques, radiation can target tumor cells more precisely and reduce the damage to normal liver cells.

1.6. Tumor marker development for HCC detection

The mortality and morbidity rates of HCC remain high despite advances in diagnostics and treatments. This is mainly because HCC patients are often diagnosed with advanced disease. Furthermore, a large proportion of these patietns have poor liver reserves due to co-existing chronic hepatitis and cirrhosis. Early detection of HCC is crucial to survival because patients with locally advanced disease or distant metastasis are not suitable for curative-intent surgical treatment. However, current diagnostic method of measuring serum AFP concentration offers low sensitivity and specificity for HCC. Thus, only less than 60% of HCC patients have elevated AFP levels whereas patients with flare up of chronic hepatitis would also have increased AFP levels. Though imaging is added to the diagnostic regimen to improve the detection accuracy of AFP, it is still a challenge to detect small tumors with size smaller than 2 cm. In this regard, researches on better HCC biomarkers have been ongoing.

Table 1.6.1. Different types of HCC tumor markers

Categories	Examples
Oncofetal antigens and glycoprotein antigens	α-fetoprotein, α-fetoprotein-L3, monosialylated α-fetoprotein and glypican-3
Enzymes and Isoenzymes	α-L-fucosidase, des-gamma-carboxy prothrombin and Golgi protein 73
Growth factors	transforming growth factor-β1 and insulin-like growth factor-II
Genes	α-fetoprotein mRNA, telomerase reverse transcriptase mRNA and hypermethylated tumor suppressor genes

(Modified from Zhou et al., 2006)

1.6.1. Oncofetal antigens and glycoprotein antigens

α-fetoprotein-L3 (AFP-L3) is one glycoform of the α-fetoprotein family named after its binding capability to the lectin *Lens culinaris* agglutin (LCA). AFL-L3 is the major glycoform present in the serum of HCC patients. It can be detected in about 35% of patients with small HCC (<3 cm) (Oka *et al*, 2001). Another study in monosialylated α-fetoprotein showed a sensitivity of 61% and a specificity of 80% in patients with moderately elevated serum AFP levels (Poon *et al*, 2002). Glypican-3 (GPC-3) is a cell-surface glycoprotein and present in a significantly higher percentage in HCC patients than in controls and cirrhosis patients. Glypican-3 can be detected in the serum of 53% HCC patients using enzyme-linked immunosorbent assay (ELISA) (Capurro *et al*, 2003).

1.6.2. Enzymes and isoenzymes

α-L-fucosidase (AFU) is a ubiquitously expressed lysosomal enzyme that hydrolyzes fucose glycosidic linkages of glycoprotein and glycolipids. Its activity is moderately elevated in HCC patients compared to patients with cirrhosis and normal individuals. It is not very useful alone but together with AFP measurement, the sensitivity can be up to 82.6% (Tangkijvanich *et al*, 1999). Des-gamma-carboxy prothrombin (DCP) is a protein induced by vitamin K deficiency and an abnormal product from liver carboxylation disturbance during the formation of thrombogen (Suzuki *et al*, 2005). It can differentiate HCC from nonmalignant hepatopathy and the sensitivity is 57% using DCP alone (Ikoma *et al*, 2002). Golgi protein 73 (GP 73) is a protein with upregulated expression in heptocytes of patients with hepatitis and cirrhosis. It had a sensitivity of 69% and a specificity of 86% with an area under the receiver operating characteristic curve of 0.79 (Marrero *et al*, 2005).

1.6.3. Growth factors

Transforming growth factor-β1 (TGF-β1) is a multifunctional cytokine involved in the regulation of growth and differentiation in both normal and transformed cells. The sensitivity for HCC of this marker is 68.4% using a cutoff level of 800 pg/mL. However, an elevated TGF-β1 level can also be observed in cirrhotic patients (Song *et al*, 2002). Insulin-like growth factor-II (IGF-II) is a tumor-specific growth factor released into the peripheral blood by tumor cells. The sensitivity of IGF-II is only 42% and it is correlated to AFP levels and thus lowers the diagnostic potential of this marker (Tsai *et al*, 2003).

1.6.4. Genetics and epigenetics – mRNA and methylation

α-fetoprotein mRNA (AFP mRNA) is found to be originated from escaped tumor cells into the circulation and correlated with high mortality rates after surgical resection. A study showed that serum AFP-mRNA quantification together with AFP can predict clinical metastasis or recurrence in 56% of patients during a 4-year follow-up (Wong *et al*, 2001). Another study of human telomerase reverse transcriptase (hTERT) mRNA by reverse-transcription-PCR reported a sensitivity and specificity of 88% and 70%, respectively. The diagnostic accuracy is proved to be superior to AFP mRNA, AFP and des-gamma-carboxy prothrombin in HCC diagnosis (Miura *et al*, 2005).

In 1999, methyated *p16* sequences were shown to be detectable in the plasma of HCC patients (Wong *et al*, 1999). Using methylation-sensitive PCR (MSP), promoter hypermethylation of the *p16* gene was observed in 73% of HCC tissues. Among the HCC patients with hypermethylation of *p16* in the tumor tissues, methylated *p16* sequences were detected in 81% of their plasma. Promoter hypermethylation of *p16* is associated with the silencing of gene expression and is an early event in carcinogenesis. The detection of aberrantly methylated TSGs in plasma represents a new approach for cancer detection (Hoque *et al*, 2006).

Chapter 2: Hypermethylation of tumor suppressor genes in cancer

2.1. Cancer epigenetics

It has long been regarded that cancer is a genetic disease characterized by germline or somatic mutations. However, since the aberration of gene methylation in cancer was discovered 25 years ago, a large body of evidences has been accumulated that suggests epigenetic changes also play an important role in cancer initiation, progression and metastasis. Epigenetics refers to a heritable change in gene expression pattern that do not involve alterations in the primary sequence of a gene (Herman & Baylin, 2003). It is shown that cancer progression involves a series of epigenetic events of which transcriptional silencing by promoter hypermethylation is considered to be an early one. Among many epigenetic phenomena, promoter hypermethylation in tumor suppressor genes has been most extensively studied.

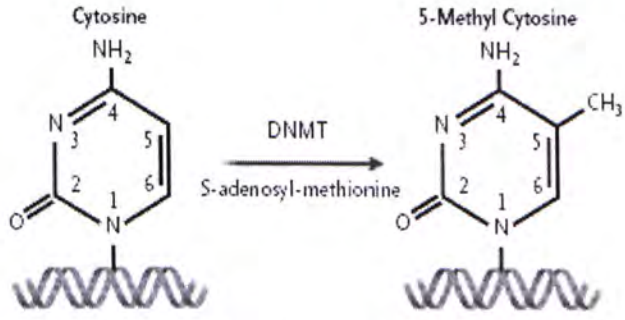

Figure 2.1.1. Pathway for the methylation of cytosine in the mammalian genome Cytosine is converted to 5-methyl cytosine catalyzed by DNA methyltransferases (DNMTs) using S-adenosyl-methionine as the methyl donor (Modified from Herman and Baylin 2003).

2.2. DNA methylation in normal cells

In mammals, DNA methylation is a covalent addition of methyl group to the 5' position of cytosine within a CpG dinucleotide using S-adenosyl-methionine as a methyl donor and catalyzed by DNA methyltransferases (DNMTs) (Herman & Baylin, 2003). Around 70% of CpG dinucleotides are methylated in the mammalian genome. The distribution of CpG dinucleotides is predominantly accumulated in small stretches of DNA of 0.5-4 kb known as CpG islands and they are typically positioned at the 5'end of genes where transcription begins (Bird, 1986). If the CpG sites in a promoter region involved in transcriptional regulation are methylated, the transcription will be blocked and this process is termed "transcriptional silencing".

DNA methylation is a very complicated process which involves a number of mediators such as enzymes, DNA-binding proteins, transcription factors and histones. The detailed mechanism of methylation is still unclear but the key process of CpG methylation is believed to be mediated by a class of enzymes termed DNA methyltransferases (DNMTs), which consist of three known biologically active enzymes in mammalian cells, DNMT1, DNMT3a and DNMT3b. DNMT3a and DNMT3b initiate *de novo* methylation and establish new DNA-methylation patterns (Okano *et al*, 1999; Okano *et al*, 1998 ; Pradhan *et al*, 1999). DNMT1 is expressed ubiquitously in somatic tissues and is preferentially active towards hemimethylated CpG sites after DNA replication (Pradhan *et al*, 1999). Studies also revealed that DNMTs may contribute to transcriptional repression in mechanisms other than methylation such as binding to other proteins like histone deacetylases (Herman & Baylin, 2003). Besides DNMTs, methyl-CpG-binding proteins (MBPs) also appear to

affect methylation-dependent gene silencing. These DNA binding proteins are specific to methylated CpG dinucleotide. To date, there are five known MBPs in mammals which are MeCP2, MBD1, MBD2, MBD4 and Kaiso (Tollefsbol, 2009). Some of the MBPs also link DNA methylation and chromatin remodeling-mediated gene silencing by associating with transcriptional repressors and recruiting histone deacetylases to methylated DNA in regions of transcriptional silencing (Jones & Baylin, 2002).

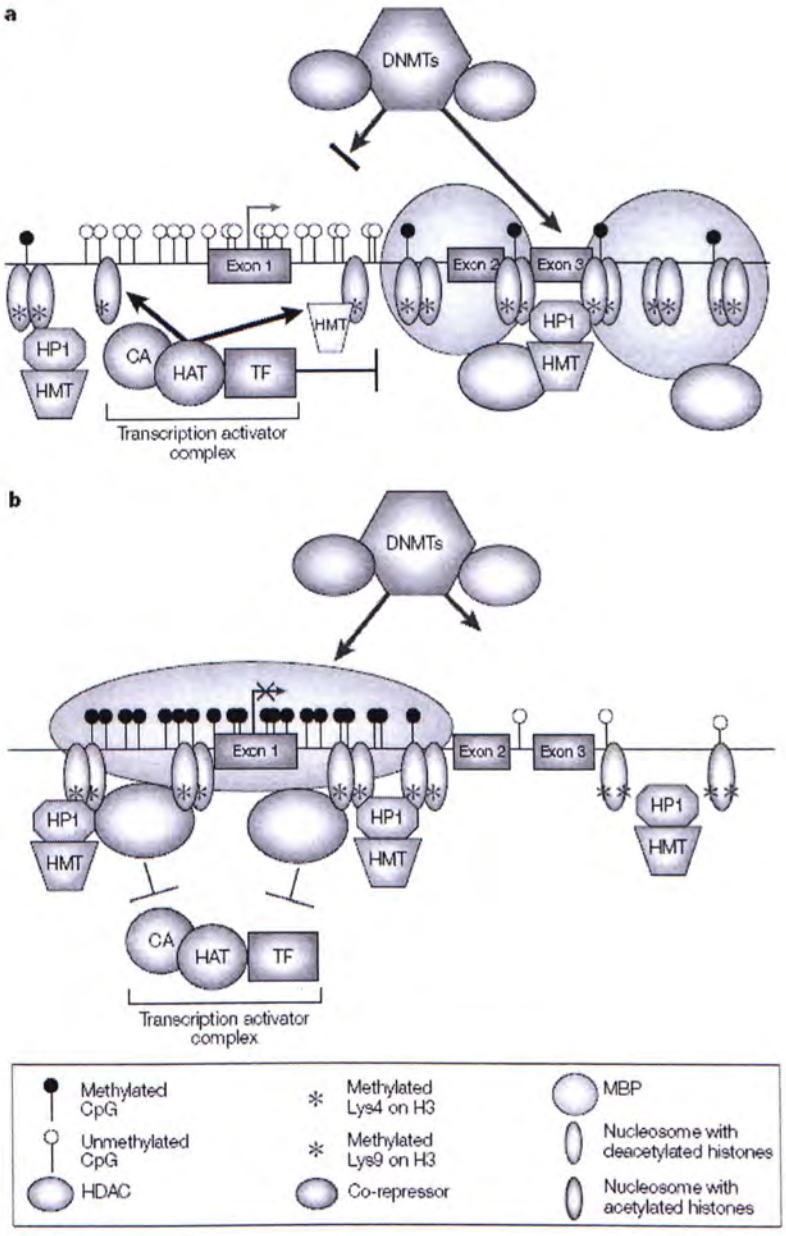

Figure 2.2.1. CpG-rich promoter in transcriptionally active and transcriptionally repressed state

(adapted from Jones and Baylin, 2002)

a. This is an unmethylated and transcriptionally permissive promoter with a CpG island. The nucleosomes with acetylated histones (ellipses shown in light green with red asterisk) are widely spaced and this type of chromatin allows the transcription activator complex to access. **b.** This is a hypermethylated and transcriptionally repressive promoter with compacted, highly deacetylated nucleosomes. This leads to transcriptional silencing. (CA, co-activator protein; HAT, histone acetyltransferase; HP1, chromodomain protein HP1α; TF, transcription factor)

2.3. Physiological role of DNA methylation in normal cells

DNA methylation usually correlates with a repressed gene expression and it can help maintain the noncoding DNA in an inert state. Hypermethylated DNA results in a late replication and consequently leads to the formation of inactive chromatin and facilitates transcriptional silencing. It is crucial to prevent the transcription of large parts of genome such as repetitive DNA, transposons or inserted viral sequences which might harm the cell (Herman & Baylin, 2003). Besides the silencing of noncoding region in the genome, other important physiological processes like X-chromosome inactivation and genomic imprinting are also mediated by DNA methylation.

X-chromosome inactivation occurs in most genes on the X chromosome. One of the two copies of these genes is silenced in females so as to compensate the increased X chromosome dosage in female cells compared with male cells (Reik & Ferguson-Smith, 2005). DNA methylation is one of the mechanisms for X-chromosome inactivation by which the selected silencing regions are transcriptionally repressed. One of the crucial events is the exclusive expression of noncoding X-(inactive)-specific transcript (*XIST*) RNA from the X chromosome to be inactivated, and hence initiates chromatin remodeling later to prevent transcription (Straub & Becker, 2007).

Genomic imprinting is defined as the epigenetic marking of parts of the genome of a diploid organism with respect to their parental origin that the imprinted genes are preferentially expressed from only one of the parental copies (Paulsen &

Ferguson-Smith, 2001). The DNA sequences responsible for establishing imprinting are named as imprinting control regions (ICRs). Differential patterns of DNA methylation in these regions may act as epigenetic marks to mediate the imprinting on neighbouring genes. Various ways have been found in different loci for monoallelic expression. One example is the *Igf2/H19* locus. This pair of genes are reciprocally expressed under the control of shared enhancer elements. The differentially methylated domain (DMD) of *Igf2* is located upstream to the *H19* promoter. On the paternal allele, the DMD acquires methylation during spermatogenesis and facilitates the enhancer to promote transcription and silence the expression of *H19*. In contrast, the hypomethylated maternal DMD is bounded by the methylation-sensitive boundary factor CTCF, which hinders the access of enhancer to *Igf2* and allows the expression of *H19* (Wood & Oakey, 2006). Imprinting errors in this region chromosome (11p15.5) are associated with the development of the Beckwith-Wiedemann syndrome (Weksberg *et al*, 2005) and Wilms tumor (Algar *et al*, 2007). Another region involved in a genomic imprinting disorder is located on chromosome 15q11-q13. Loss of paternal contribution in this locus results in the Prader-Willi syndrome while loss of maternal contribution leads to the development of Angelman syndrome (Glenn *et al*, 2000).

2.4. Aberrant DNA methylation in cancer

There are two major epigenetic disruptions in cancer. The first one is DNA hypomethylation of repetitive sequences, noncoding DNA, the inactive X-chromosome and imprinted regions; and the second one is DNA hypermethylation in the promoters of tumor suppressor genes.

2.4.1. DNA hypomethylation in cancer

Global DNA hypomethylation is one of the earliest epigenetic alterations discovered in human cancers (Feinberg & Tycko, 2004). During carcinogenesis, the degree of hypomethylation of genomic DNA is increased with the stage of the tumor progression. More frequent mitotic recombination by hypomethylation results in chromosomal rearrangements, deletions and translocations and thus would affect the stability of the chromosomes. In addition, those previously silenced regions such as long interspersed nuclear elements 1 and *Alu* sequences may be reactivated and leads to the expression of inserted viral genes or imprinted genes on the inactive X-chromosome (Esteller, 2008). Some oncogenes are shown to be activated such as the hypomethylation of *HpaII* sites in the 3' region of *H-Ras* found in non-small cell lung cancer (Vachtenheim *et al*, 1994). As another example, promoter hypomethylation of the *c-myc* gene has also been found in several tumor cell lines (Cheah *et al*, 1984) .

2.4.2. DNA hypermethylation in cancer

Promoter hypermethylation of tumor suppressor genes is regarded as an early event in the pathogenesis of cancers. DNA hypermethylation has resulted in the transcriptional repression of tumor suppressor genes and DNA repair systems. Knudson's two-hit hypothesis (Knudson, 2001) postulates that for the function of a tumor suppressor gene to be disrupted, it requires a complete loss of function of both copies of the involved gene. Aberrant promoter methylation is an important event that can be the first hit or the second hit in carcinogenesis. For a tumor suppressor gene, mutation in coding regions can occur in inherited cancer or sporadic cancer to

constitute the first hit while promoter hypermethylation can occur in somatic cancer to constitute the first hit. In an inherited cancer, chromosomal deletions involving the second copy or promoter hypermethylation can be the second hit in tumors while in somatic cancers, chromosomal deletions often constitutes the second hit to eliminate the remaining gene copy (Herman & Baylin, 2003). Promoter hypermethylation has been demonstrated in many tumor suppressor genes such as *p16* (*cyclin-dependent kinase inhibitor 2A*), *VHL* (gene associated with von Hippel-Lindau disease), *APC* (*adenomatosis polyposis coli*) and *BRCA1* (b*reast-cancer susceptibility gene 1*) (Esteller *et al*, 2000a; Esteller *et al*, 2000b; Herman *et al*, 1994; Merlo *et al*, 1995). Compared with hypomethylation, hypermethylation is studied more extensively of its role and their diagnostic potential in different cancers.

2.5. Development of methylation markers in tumor diagnosis

The development of better tumor markers may be useful for reducing the mortality of cancer as a large proportion of cancers are discovered at an incurable stage. A number of studies have investigated the clinical potential of novel tumor markers in disease stratification, progress monitoring and prognostication. A cancer biomarker can be any cellular, biochemical, molecular or genetic alterations indicating the presence of the tumor in the body. It can be tumor-derived DNA, RNA and protein which is present in a detectable form in circulation (Hanash *et al*, 2008; Marrero & Lok, 2004). Current noninvasive markers in clinical use for cancer diagnosis are mainly proteins that are secreted by tumor cells. However, only a subset of cancers produce specific proteins that are detectable in the circulation (Chan & Lo, 2007). RNA has also been studied through microarray analysis but its use as a biomarker is

limited by its relative instability of RNA compared with DNA in circulation. Therefore, the chemical and biological stability of DNA makes it appealing to be developed as cancer biomarkers (Tollefsbol, 2009). One of the most widely studied approach to detect circulating tumoral DNA is based on the detection of promoter hypermethylation of TSGs. Advances in molecular technology have provided various approaches for the sensitive detection of DNA methylation patterns and opened up the potential of utilizing circulating methylated DNA as cancer biomarkers.

2.5.1. Methods for the analysis of DNA methylation markers

Bisulfite conversion and methylation-sensitive restriction enzyme digestion are the two most commonly used methods for studying DNA methylation in different tissues (Frommer *et al*, 1992; Mcclelland, 1981). Restriction landmark genomic scanning (RLGS) is one of the earliest methods for studying genome-wide DNA methylation patterns (Costello *et al*, 2000). DNA is digested by methylation-sensitive restriction enzymes and subsequently radioactive-labeled on unmethylated CpG sites, then subjected to size-fractionation in one dimension using gel electrophoresis. Next, a second enzyme specific for a high-frequency target is added to the products, and the fragments are separated in another dimension to produce a group of scattered methylation hot-spots. The hot-spot pattern is compared between normal and tumor samples so that the frequency and location of methylated sites can be revealed by the position and intensity of the spots.

The invention of bisulfite-conversion has revolutionized the analytical methods used for DNA methylation analysis. Sodium bisulfite can convert unmethylated cytosines to uracils while the methylated cytosines remain unaffected (Frommer *et al*, 1992).

Bisulfite genomic sequencing (Frommer *et al*, 1992), combined bisulfite restriction analysis (COBRA) (Xiong & Laird, 1997) and methylation sensitive single nucleotide primer extension (Ms-SNuPE) (Gonzalgo & Jones, 1997) utilize primers that do not cover any potential methylated sites and determine the methylation status of the region by analyzing the sequences within the amplicon (Laird, 2003). The development of methylation-specific PCR (MSP) (Herman *et al*, 1996) has greatly enhanced the study of DNA methylation as it allows the detection of aberrant DNA methylation in small amounts of DNA template obtained from clinical samples. The design of a MSP primer set is to amplify specifically the methylated DNA or unmethylated DNA in bisulfite-treated samples. Quantitative analysis of methylated sequences by real-time MSP (Lo *et al*, 1999) and Methylight (Eads *et al*, 2000) have also been developed.

2.5.2. Detection of tumor-associated methylated DNA in the circulation of cancer patients

The detection of tumor-derived aberrant DNA methylation has evolved as a new approach for cancer detection. In addition to detecting such aberrant methylation in tumor tissues, detection of such sequences in other biological samples, in particular plasma/serum has been attempted. However, the detection of tumor-associated aberrantly methylated TSG sequences in plasma/serum is technically challenging because these sequences are typically present at very low concentrations (Wong *et al*, 2003) and among a high concentration of background wild-type sequences derived mainly from blood cells (Jahr *et al*, 2001).

In earlier studies, MSP-based methods have been applied for detecting these

tumor-derived methylated sequences in the circulation of cancer patients. For example, methylated *p16* (Wong *et al*, 2003) and *RASSF1A* (Yeo *et al*, 2005) sequences were detected in the circulation of HCC patients. Methylated *GSTP1* sequences were detected in the circulation of prostate cancer patients (Goessl *et al*, 2000). Methylated *APC* sequences were detected in esophageal cancer patients (Kawakami *et al*, 2000). Methylated *DAPK* sequences were detected in the serum of breast cancer patients (Dulaimi *et al*, 2004). As different types of cancers might have distinct profiles of aberrant TSG methylation, such profiles might be developed as specific tumor markers for certain cancers. Moreover, the combination of different TSG methylation markers might be useful for more sensitive cancer detection.

It was reported that the pattern of CpG island methylation of a cancer was tumor-specific (Costello *et al*, 2000) and a number of aberrantly methylated tumor suppressor genes are frequently observed in HCC tissues. TSGs that are commonly methylated in HCC include *p16INK4A* (Lo *et al*, 1999; Wong *et al*, 1999; Wong *et al*, 2003), *RASSF1A* (Honda *et al*, 2008; Yeo *et al*, 2005; Zhong *et al*, 2003), *GSTP1* (Su *et al*, 2007; Yang *et al*, 2003; Zhong *et al*, 2002), *APC* (Nishida *et al*, 2008; Nishida *et al*, 2007; Yang *et al*, 2003) and *SOCS1* (Miyoshi *et al*, 2004; Nagai *et al*, 2002; Yoshikawa *et al*, 2001). The functions of these genes are discussed in more detail below.

Glutathione S-transferase Pi (GSTP1) is one of the members of the glutathione S-transferase family which protects cells against cytotoxic and carcinogenic agents like oxidants and electrophilic carcinogens (Mannervik *et al*, 1985). It catalyzes the conjugation of glutathione with electrophilic carcinogens and produces less cytotoxic

and more readily excreted metabolites (Zhong *et al*, 2002). Accumulation of electrophilic metabolites after the loss in *GSTP1* had been observed in prostate and resulted in DNA damage and mutation (Lee *et al*, 1994). As the liver is functioning as a detoxifying organ of the body, loss of *GSTP1* may further facilitate the exposure of toxic metabolites to hepatocytes and enhance the transformation of hepatocytes by tumor inducers (Su *et al*, 2007). In HCC, the methylation frequency of *GSTP1* in tumor tissue ranges from 41% to 88.5% (Lee *et al*, 2003; Su *et al*, 2007; Wang *et al*, 2006; Zhang *et al*, 2005; Zhong *et al*, 2002).

Suppressor of cytokine signalling-1 (SOCS1) is a member of SOCS protein family which is a negative regulator of the Janus kinase (JAK) and the signal transducer and activators of signaling (STAT) pathways. It binds to JAK directly or indirectly and inhibits the phosphorylation of STAT and downregulates the expression of target genes (Starr *et al*, 1997). In HCC, the previously reported methylation frequency of *SOCS1* in HCC tissue ranges from 41% to 65% (Miyoshi *et al*, 2004; Okochi *et al*, 2003; Yang *et al*, 2003; Yoshikawa *et al*, 2001).

Adenomatous polyposis coli (APC) is a negative regulator of the Wnt signaling pathway and is also involved in cell migration and adhesion, transcriptional activation, and apoptosis. Loss of APC results in accumulation of β-catenin and interaction with the lymphoid enhancer factor-T cell factor (LEF-TCF) family of transcription factors and promotes the cells to enter the cell cycle (Csepregi *et al*, 2008). Hypermethylation of *APC* is very common in HCC with high methylation frequency in tumor tissues ranging from 53% to 88.3% (Csepregi *et al*, 2008; Katoh *et al*, 2006; Lee *et al*, 2003; Nishida *et al*, 2008; Yang *et al*, 2003).

p16INK4a (cyclin-dependent kinase inhibitor 2A, p16) is one of the cell cycle regulator and inhibits the proliferation of normal cells by binding to CDK4 and CDK6. It prevents the interaction of CDK4 and CDK6 with cyclin D and hence also prevents the phosphorylation of retinoblastoma protein (pRb) and results in inactivation (Azechi *et al*, 2001; Maeta *et al*, 2005). The hypermethylation of *p16* is widely studied and the methylation frequency was observed from 16 to 79.5% (Katoh *et al*, 2006; Lee *et al*, 2003; Nishida *et al*, 2008; Su *et al*, 2007; Wong *et al*, 1999; Yang *et al*, 2003; Zhang *et al*, 2007).

Most studies have used MSP as the technique to detect hypermethylated tumor suppressor genes in plasma or serum. However, a wide range of sensitivities of approximately 20-80% is observed whereas the reported frequency of hypermethylation in HCC tissues is 50-90%. It is believed that the sodium bisulfite treatment in MSP that leads to substantial degradation of DNA (up to 96%) (Grunau *et al*, 2001) and the presence of low concentrations of circulating tumor DNA in cancer patients are the reasons for the unsatisfactory detection rate of such sequences in plasma/serum (Chan *et al*, 2008a; Chan & Lo, 2007).

Recently, a non-bisulfite-based technique termed methylation-sensitive restriction enzymes mediated real-time quantitative PCR was developed to detect methylated *RASSF1A* sequences quantitatively in maternal plasma (Chan *et al*, 2006a) and the plasma of HCC patients (Chan *et al*, 2008a). Although this technique showed a substantial improvement of detection rate in HCC of 93%, low concentrations of methylated *RASSF1A* were also detected in chronic HBV carriers. Thus, for HCC

surveillance purpose, it is hoped that one could further enhance the specificity of this approach.

2.6. Aim of thesis

To date, the measurement of serum AFP level and the imaging of liver by ultrasound represent the most common regimen for HCC detection. Low diagnostic accuracy of the diagnostic approach prompts researchers to search for more accurate markers for early HCC detection which can eventually improve the clinical outcomes and survival rates.

Aberrant methylation of tumor suppressor genes has been found in the plasma/serum of patients with different cancers (Laird, 2003). Multiple markers have been shown to enhance the detection rates (Hoque *et al*, 2006). In this thesis, I developed a panel of methylated markers including *GSTP1*, *SOCS1*, *APC* and *p16* that involved in multiple cellular pathways by methylation-sensitive restriction enzymes mediated real-time PCR for the detection of HCC.

SECTION II: MATERIALS AND METHODS

Chapter 3: Methods for detecting DNA methylation

3.1. Subject recruitment

Fifty-six HCC patients were recruited with informed consent from the Department of Surgery, Prince of Wales Hospital, Shatin, Hong Kong. The diagnosis of HCC was histologically confirmed. Six milliliters of peripheral blood were collected into two ethylenediaminetetraacetic acid (EDTA) tubes from each patient. A total of 90 blood specimens were obtained from the 56 HCC patients of which 56 were collected 1 hr before surgical resection of the tumor and 34 were at one month postoperatively. Fifty-five chronic carriers of hepatitis B virus (HBV) infection and 58 healthy volunteer with matched age (within 5 years) and sex were recruited as controls.

3.2. Sample collection and processing

3.2.1. Tumor tissue samples

The tumor tissues were fresh frozen in liquid nitrogen immediately after collection and stored at -80°C until further analysis.

3.2.2. Peripheral blood samples

The blood samples in EDTA tubes were processed within six hours after collection (Chan *et al*, 2005a). They were centrifuged at 1,600 *g* for 10 min at 4°C (Centrifuge 5810R, Eppendorf, Hamburg, Germany) to separate plasma and blood cell layers.

Plasma was then carefully transferred to a 2 mL polypropylene tubes and microcentrifuged at 16,000 *g* for 10 min at 4°C (Centrifuge 5415R, Eppendorf) (Chiu *et al*, 2001). The supernatant was transferred to a new 1.5 mL polypropylene tube and stored at -20°C. The buffy coat was recentrifuged at 2,500 *g* for 5 min at room temperature. Residual plasma was removed and the sample was stored at -20°C.

3.3. DNA extraction

3.3.1. Plasma samples

DNA was extracted from the plasma samples using the QIAamp DSP DNA Blood Mini Kit (Qiagen, Hilden, Germany) according to the manufacturers' protocol. Briefly, 800 μL of plasma sample was processed and split into two tubes of 400 μL plasma each time to facilitate the extraction process. 400 μL of plasma was added to 40 μL of Qiagen protease and 400 μL Lysis buffer was added subsequently. The lysate was vortexed and incubated at 56°C for 10 min. 400 μL chilled 100% ethanol was added and mixed to precipitate the DNA. The lysate was processed by either the spin protocol or the vacuum protocol provided by manufacturer. For the spin protocol, the column was placed in a collection tube and centrifuged at 16,000 *g* for 1 min until all the lysate passed through the membrane. Five hundred microliters of the AW1 wash buffer were added and centrifuged at 16,000 *g* for 1 min to wash the column. This process was repeated except that the AW1 buffer was replaced by the AW2 buffer. The column was centrifuged again at 16,000 *g* for 2 min to remove any residual buffer to avoid carryover to downstream analysis. For the vacuum protocol, the column was inserted into the VacConnector (VC) on the vacuum system. Six

hundred microliters of the lysate were then added to the QIAamp Mini Spin column. This process was repeated until all lysate of a particular sample has been loaded onto the colulmn. The main vacuum valve was open and the lysate was sucked by the vacuum to pass through the membrane and drain into the vacuum manifold. The column was then washed with the AW1 and AW2 buffer sequentially. Next, the column was placed into a collection tube and centrifuged at 16,000 *g* for 2 min to remove any residual buffer. DNA was eluted with 50 μL distilled water and stored at -20°C.

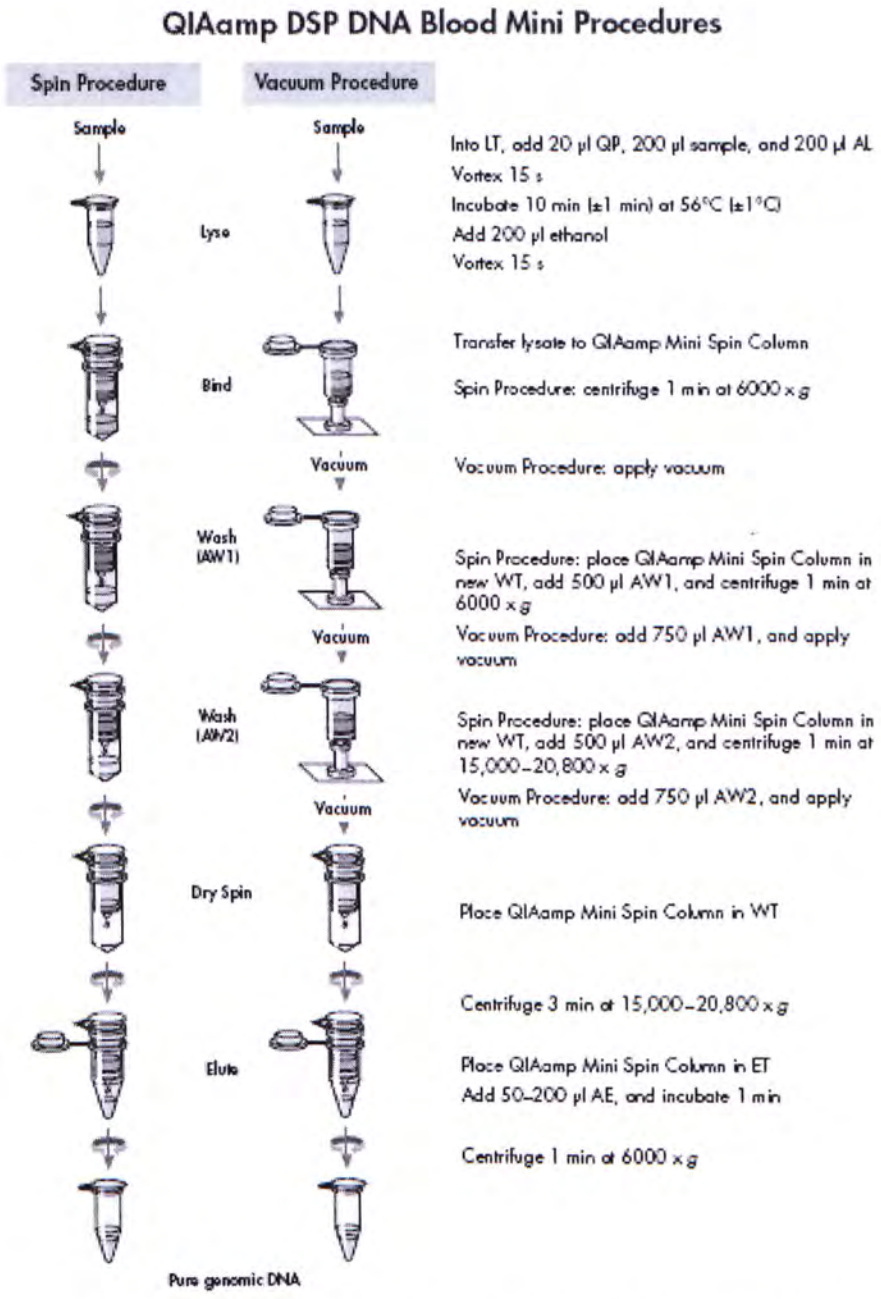

Figure 3.3.1. The extraction procedure by QIAamp DSP DNA blood mini kit (Adapted from Qiagen's kit manual)

3.3.2. Blood cells

Blood cell DNA was extracted using QIAamp DNA Blood Mini Kit (Qiagen, Hilden, Germany) according to the manufacturer's spin protocol. 400 µL of blood cells was added to 40 µL of Qiagen protease and 400 µL Lysis buffer was added afterwards. The lysate was vortexed and incubated at 56°C for 10 min. 400 µL chilled 100% ethanol was added and mixed to precipitate the DNA. The entire lysate was then transferred to a QIAamp Mini Spin column which was placed in a collection tube and centrifuged at 16,000 *g* for 1 min until all the lysate passed through the membrane. 500 µL AW1 and AW2 wash buffer were added and centrifuged at 16,000 *g* for 1 min to wash the column subsequently. The column was centrifuged again at 16,000 *g* for 2 min to eliminate any residual buffer to avoid inhibition or contamination of the downstream assay. DNA was eluted twice with 50 µL distilled water and stored at -20°C.

3.3.3. Tumor tissue

Tissue DNA was extracted using a QIAamp DNA Mini Kit (Qiagen, Hilden, Germany) according to the manufacturer's tissue protocol. A small piece of tumor tissue was lysed with 180 µL buffer ATL and 20 µL proteinase K at 56°C overnight on a rocking platform. The lysate was then incubated with 200 µL at 70°C for 10 min. 200 µL chilled 100% ethanol was added and mixed to precipitate the DNA. The entire lysate was then transferred to a QIAamp Mini Spin column which was placed in a collection tube and centrifuged at 16,000 *g* for 1 min until all the lysate passed through the membrane. Five hundred microliters of AW1 wash buffer were added and centrifuged at 16,000 *g* for 1 min to wash the column. Then, this process was repeated with the AW1 buffer replaced by the AW2 buffer. The column was

centrifuged again at 16,000 *g* for 2 min to eliminate any buffer carryover to avoid inhibition or contamination of the downstream assay. DNA was eluted twice with 50 μL distilled water and stored at -20°C.

3.4. Quantitative analysis of methylated DNA using methylation-sensitive restriction enzyme-mediated real-time quantitative PCR (MSRE-qPCR)

3.4.1. Methylation-sensitive restriction enzyme-mediated real-time quantitative PCR

MSRE-qPCR is a non-bisulfite-based method for detecting hypermethylated DNA in a sample (Chan *et al*, 2008a). The DNA samples were first subjected to methylation-sensitive restriction enzymes (MSRE) digestion before real-time PCR (qPCR). When the cytosine residue of a MSRE recognition site is methylated, the digestion by the MSRE is blocked, thus, leaving an intact DNA template for downstream PCR amplification. However, if the cytosine is not methylated, the sequence is cut and no amplification of the target would be resulted (Figure 3.4.1).

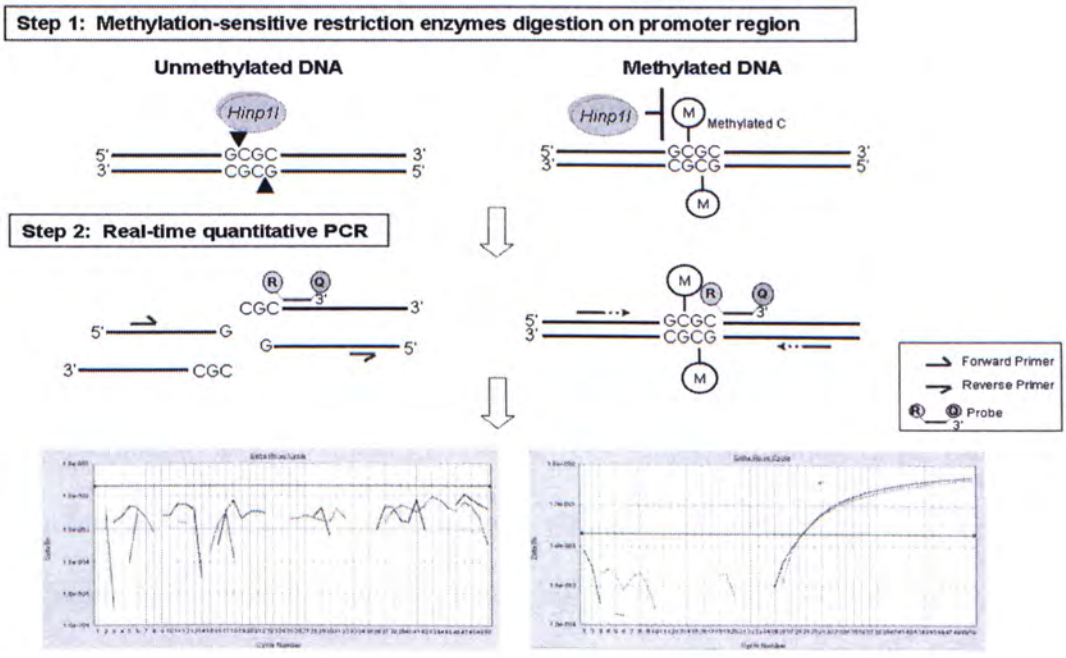

Figure 3.4.1. Schematic diagram of MSRE-qPCR

3.4.2. Principle of real-time quantitative PCR

Real-time quantitative polymerase chain reaction (real-time PCR / qPCR) is a modification of conventional polymerase chain reaction (PCR) and allows the quantification of the initial amount of the target DNA in the sample. The original real-time PCR was performed with the addition of a fluorescence dye binding specifically to double-stranded DNA, for example ethidium bromide or SYBR Green I. The intensity of the fluorescent signal would increase with the amount of double-stranded DNA formed. However, this method cannot differentiate the amplification of the desired product from non-specific amplification. To overcome this problem, TaqMan Probe-based technology was developed (Gibson *et al*, 1996). This method involves a dual-labeled single-stranded oligonucleotide probe with a fluorescent reporter dye on the 5' end and a quencher on the 3' end. If the probe remains intact, the reporter and quencher are close to one another and the fluorescence emitted by the reporter is reduced by fluorescence resonance energy transfer (FRET). On the other hand, if the target sequence is present, the probe annealing to it is cleaved by the 5' nuclease activity of the *Taq* DNA polymerase during extension. This cleavage separates the reporter from the quencher and results in an increase in fluorescence signal. The fluorescence signal intensity generated would be proportional to the amount of the amplicons produced and hence reflects the quantity of the nucleic acid target.

3.4.3. Real-time PCR primer design

There are several steps for designing real-time assays for quantitative analysis of methylated DNA in the plasma of HCC patients. First, I identified the appropriate targets which are the promoter regions of tumor suppressor genes that are frequently

methylated in HCC. After identifying the appropriate tumor suppressor genes, restriction maps of their promoter regions were constructed to show the restriction sites of common methylation-sensitive restriction enzymes using the UCSC Genome Browser (University of California, Santa Cruz).

Using these restriction maps, I identified regions that contain four or more restriction sites within 200 bp. The presence of four or more restriction sites within a PCR amplicon can increase the chance of cutting an unmethylated sequence whereas the length requirement is to increase the sensitivity of detecting tumoral DNA in plasma as these sequences have been shown to be predominantly below 200 bp (Chan & Lo, 2006).

After the design of the real-time PCR systems for detecting the methylated TSG, assays for ascertaining the completeness of restriction enzymes digestion were also developed. These assays were designed on the promoter of the β-actin gene (*ACTB*) which was previously reported to be completely unmethylated. The control assays had similar amplicon lengths and number of restriction sites as the corresponding TSG assays. If the enzyme digestion is complete, the unmethylated *ACTB* sequences should not be detectable and the result of the TSG detection would be used for further analysis. On the other hand, the presence of detectable unmethylated *ACTB* sequences would indicate incomplete digestion and the enzyme digestion step would need to be repeated.

In this thesis, real-time PCR assays are named by their gene names such as *GSTP1*, *SOCS1*, *APC* and *p16*; and for the internal control assays, they are named as

β-actin*gstp1 control, β-actin*socs1 control, β-actin*apc control and β-actin*p16 control to represent the internal control amplicon/assay of *GSTP1, SOCS1, APC* and *p16* assay, respectively.

One mock digestion control using genomic DNA from healthy individual was included in each round of digestion to ensure the digestion condition was normal. The final optimized digestion conditions are listed in table 3.4.2.

Table 3.4.1. Number of restriction sites in each assay

Amplicon		Combination of restriction enzymes	Total no. of restriction sites
GSTP1	Target	**Bsh1236I + HinpII*	6
	Actin control		7
SOCS1	Target	*Bsh1236I + HinpII*	10
	Actin control		9
APC	Target	*AciI + HinpII*	6
	Actin control		5
p16	Target	*AciI*	5
	Actin control		4

* *HinpII* and *AciI* were supplied by New England Biolabs and *Bsh1236I* was from Fermentas.

Table 3.4.2. Summary of the digestion conditions

GSTP1		***SOCS1***	
10x NEB buffer 4	1x	10x NEB buffer 4	1x
HinpII	12 U	*HinpII*	10 U
Bsh1236I	12 U	*Bsh1236I*	10 U
Plasma DNA or 50 ng tissue DNA	20 µL	Plasma DNA or 50 ng tissue DNA	20 µL
Water	0.1 µL	Water	0.5 µL
Total volume	25 µL	Total volume	25 µL
Incubation time	16 hrs	Incubation time	16 hrs
APC		***p16***	
10x NEB buffer 3	1x	10x NEB buffer 3	2.8 µL
AciI	60 U	*AciI*	40 U
HinpII	60 U		
Plasma DNA or 50 ng tissue DNA	20 µL	Plasma DNA or 50 ng tissue DNA	20 µL
Total volume	35.5 µL	Total volume	26.8 µL
Incubation time	16 hrs	Incubation time	28 hrs

3.4.4. Duplex real-time PCR

Duplex real-time PCR was used to co-amplify the target genes and the internal control. This approach enabled the simultaneous detection of the internal control *ACTB* and the target TSG sequences in a sample such that the enzyme digestion efficiency of a particular sample can be accurately analyzed. Moreover, this design can also improve the robustness of the analysis and reduce the reagent cost. In my study, TaqMan probes with non-fluorogenic quenchers (NFQ) were used. The advantage of non-flourogenic quenchers compared with fluorogenic quenchers e.g. TAMRA™ (6-carboxyteramethylrhodamine) include a lower background noise and better sensitivity. Probes labeled with FAM™ (6-carboxyfluorescein) (λ_{max} = 518 nm) are used in assays detecting the methylated TSGs and probes labeled with VIC® (λ_{max} = 554 nm) are used in the digestion control assays. A standard curve of calibrators ranging from 10,000 copies per 5 µL to 2.4 copies per 5 µL was prepared by serial dilutions of a known quantity of human blood cell DNA from a healthy control sample. All the real-time PCR assays were performed using an Applied Biosystems 7300 Sequence Detector (Applied Biosystems, Foster City, CA). All sample wells in a sealed 96-well plate were illuminated with a tungsten-halogen lamp and the fluorescence emission was detected through four filters onto a charge-coupled device (CCD) camera. ROX dye (λ_{max} = 610 nm) was used as passive reference to normalize for non-PCR-related fluctuations in fluorescence signal. The real-time PCR data were analyzed by the Sequence Detection System (SDS) Software v1.2.3 (Applied Biosystems, Foster City, CA). The threshold cycle (C_T) was determined for each well and a standard curve was constructed by plotting the C_T against the quantity of the corresponding calibrators.

3.4.5. Real-time detection of GSTP1, SOCS1, APC, p16 and ACTB sequences

Hypermethylated *GSTP1, SOCS1, APC and p16* sequences, together with the respective *ACTB* digestion control sequences were detected using the methylation-sensitive restriction enzymes-mediated real-time PCR. The assays were performed using the TaqMan® Universal PCR Master Mix (Applied Biosystems, Foster City, CA) in a total reaction volume of 50 μL. The PCR Master Mix was optimized for TaqMan reactions and contained AmpliTaq Gold DNA polymerase, AmpErase UNG, dNTPs, passive reference ROX and optimized buffer components. The primer and probe concentrations for each assay were optimized with blood cells DNA from healthy individuals and universal methylated DNA (Chemicon) and were listed in table 3.4.4. The thermal profile of the real-time PCR was 50°C for 2 min, 95°C for 10 min and 50 cycles of 95°C for 15 sec and 60°C for 1 min. All the samples were run in duplicates and the mean quantities were used for downstream analysis. No template controls were included in all reaction plates to detect any DNA contamination in reaction components.

3.4.6. Statistical analysis of real-time PCR results

Demographical information of HCC patients and HBV carriers were analyzed by the Student's t test, chi-square analysis and the Mann-Whitney U test. The concentrations of tumor suppressor genes in the plasma of HCC patients, HBV carriers and healthy controls were compared by the Kruskal-Wallis test. The methylated TSG concentrations of preoperative and postoperative plasma in HCC patients were compared using the Wilcoxon signed-rank test. The differences between survival curves were analyzed by the log-rank test and the associations between clinical parameters and TSG methylation with survival rates were analyzed

using univariate and multivariate Cox regression analyses. Survival analyses were done by MedCalc version 9.6.4 and other statistical analyses were performed by the SigmaStat 3.5 software.

Table 3.4.3. Primer and probe sequences of quantitative real-time PCR

Gene	Oligonucleotide	Sequence (5' to 3')	Product length (bp)
GSTP1			
	GSTP1-666F	GCAGCGGTCTTAGGGAATTTC	171
	GSTP1-836R	CTGGAGTCCCCGGAGTCG	
	GSTP1-689T	FAM-CCCGCGATGTC-NFQ	
SOCS1			
	SOCS1-1879F	CGTTCGCACGCCGATTAC	176
	SOCS1-2053R	CGCTAAGGGCGAAAAAGCA	
	SOCS1-2009T	FAM-TGGTGCGCGACAG-NFQ	
APC			
	APC_B-864F	GAGAGAGAAGCAGCTGTGTAATCC	164
	APC_B-1027R	TCCGGCAGCACCTCCAT	
	APC_B-894T	FAM-TGCGGACCAGGGCG-NFQ	
p16			
	p16_2_01F	CTGGCTGGTCACCAGA	98
	p16_2_01R	CCGGCTCCATGCTGCTC	
	p16_2_01T	FAM-CGGACCGCGTGCGCT-NFQ	
β-actin*gstp1 control			
	actb-gstp1-01F	GCGCCGTTCCGAAAGTT	137
	actb-gstp1-01R	CGGCGGATCGGCAAA	
	actb-gstp1-01T	VIC-CCGAGACCGCGTC-NFQ	
β-actin*socs1 control			
	actb-socs1-01F	TTCGCCCGTGCAGAGC	176
	actb-socs1-01R	CGAGAGCGGCACCCC	
	actb-socs1-01T	VIC-ACACCCCACGCCAGTT-NFQ	
β-actin*apc control			
	actb-apc-01F	ACGGCTCCGGCATGTG	162
	actb-apc-01R	GGCTCCTGTGCAGAGAAAGC	
	actb-apc-01T	VIC-CCCCAGGCACCAGGTA-NFQ	
β-actin*p16 control			
	actb_p16_2_01F	CCACGCCAGTTCGGAGG	92
	actb_p16_2_01R	AGAGCCCGGCTCAGACAAA	
	actb_p16_2_01T	VIC-CTCGGGAGGCGCGCT-NFQ	

Notes
F: Forward primer
R: Reverse primer
T: Fluorescent probe
NFQ: Minor-groove binding non-fluorescent quencher

Table 3.4.4. Real-time PCR reaction conditions for quantitative analysis of tumor suppressor genes

Target gene	*GSTP1*		*SOCS1*		*APC*		*p16*	
Actin control	*β-actin*gstp1 control*		*β-actin*socs1 control*		*β-actin*apc control*		*β-actin*p16 control*	
Reaction Component	**Volume per reaction (µL)**	**Final concentration**	**Volume per reaction (µL)**	**Final concentration**	**Volume per reaction (µL)**	**Final concentration**	**Volume per reaction (µL)**	**Final concentration**
TaqMan Universal PCR Master Mix (2X)	25	1X	25	1X	25	1X	25	1X
Forward primer of target gene (10µM)	3	600 nM	2.5	500 nM	2.1	420 nM	2.25	450 nM
Reverse primer of target gene (10µM)	3	600 nM	2.5	500 nM	2.1	420 nM	2.25	450 nM
TaqMan Probe of target gene (10uM)	1	200 nM	0.65	130 nM	0.7	140 nM	0.5	100 nM
Forward primer of actin control (10uM)	1.25	250 nM	1.25	250 nM	2.1	420 nM	1.5	300 nM
Reverse primer of actin control (10uM)	1.25	250 nM	1.25	250 nM	2.1	420 nM	1.5	300 nM
TaqMan Probe of actin control (10uM)	0.35	70 nM	0.3	60 nM	0.7	140 nM	0.35	70 nM
Water	5.15	-	6.55	-	1.2	-	3.65	-
Digestion mixture of DNA	10	-	10	-	14	-	13	-
Total	50		50		50		50	

Table 3.4.5. Thermal profile for qPCR analysis

Thermal Cycler	Times and Temperatures			
	First cycle		Each of 50 cycles	
			Denaturation	Anneal/Extend
ABI Prism 7300 Sequence Detector	2 min	10 min	15 sec	1 min
	50°C	95°C	95°C	60°C

(Modified from TaqMan Universal PCR Master Mix Protocol)

3.5. Methylation study of *GSTP1, SOCS1, APC, p16* and *ACTB* in tumor tissues and blood cells using bisulfite sequencing

3.5.1. Principle of bisulfite modification

Bisulfite modification is widely used in methylation analysis, which utilizes sodium bisulfite to deaminate unmethylated cytosine to uracil while the 5-methylcytosine remains unchanged (Frommer *et al*, 1992). After bisulfite treatment and PCR, the methylation status of CpG sites can be determined. Bisulfite conversion works by reaction between cytosine and bisulfite ion to form a sulphonated cytosine derivative. The reaction is reversible and affected by the concentration of hydroxide, bisulfite ion and temperature.

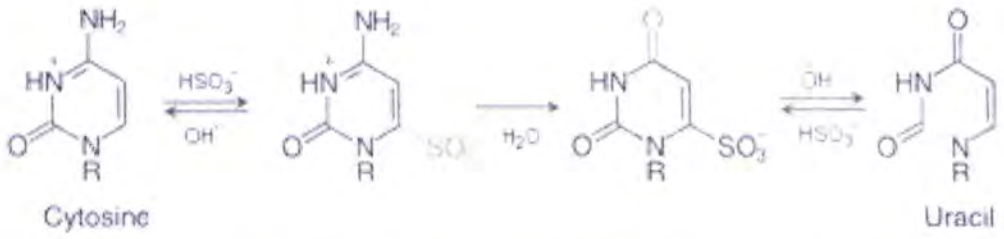

Figure 3.5.1. The chemical reaction of sodium bisulfite conversion of unmethylated cytosine
(Adapted from http://www.dkfz.de/funct_genome/epigenetics-genotyping.html)

A uracil-bisulfite derivative is formed after hydrolytic deamination. This reaction requires a catalyst like sulfite, bisulfite or acetate anions. Lastly, uracil is obtained by adding alkaline substances to remove the sulphonate group on the fifth carbon. This reaction can occur when cytosine is a free base, nucleoside (ribo- or deoxyribo-), nucleotide or oligonucleotide. After PCR amplification, the

unmethylated cytosine (appears as uracil) in the bisulfite-treated DNA is amplified as thymine while the methylated cytosine remains as cytosine. Hence, the methylation status of a sample can be determined by analyzing the sequence of the bisulfite-converted DNA.

3.5.2. Bisulfite conversion

Bisulfite conversion of DNA samples were performed using the EZ DNA Methylation Kit (Zymo Research, Orange, CA) according to the manufacturer's protocol. Five microliters of the M-Dilution Buffer were incubated at 37°C for 15 min with 1 μg of tissue DNA or blood cells DNA after adjusting to a total volume of 50 μL with deionized water. Then the sample was mixed with 100 μL freshly prepared CT Conversion Reagent and incubated in the dark at 56°C for 16 hr. The sample was subsequently cooled on ice for 10 min. Four hundred microliters of M-Binding Buffer was mixed with the sample and the mixture was loaded onto a Zymo-Spin IC Column and centrifuged at 13,000 rpm for 30 s. 100 μL of M-Wash Buffer was added to wash the column which was then centrifuged at full speed for 30 s. Then 200 μL of M-Desulphonation Buffer was loaded to the column and followed by incubation at room temperature for 15 min. After centrifugation at full speed for 30 s, 200 μL M-Wash Buffer was added twice sequentially to wash away the residual buffer. Finally, the bisulfite-converted DNA was eluted with 25 μL of 1:1 mixture of M-Elution Buffer and deionized water.

3.5.3. Sequencing primer design

As the aim of bisulfite sequencing was to build the foundation for testing the capability of real-time PCR assay in reflecting the actual methylation status in tumor

tissue and bood cells, the bisulfite PCR was designed to sequence the regions corresponding to the amplicons of the real-time PCR assays. In addition, owing to the limitation in sequencing that the first and last 50-100 bp of the PCR amplicon is usually not able to be sequenced or at a very low resolution, therefore, the bisulfite PCR was designed from 100 bp upstream to 100 bp downstream of the amplicon if possible in order to obtain the complete sequences. As the two parental DNA strands are no longer complementary to each other after bisulfite conversion, suitable primers may be obtained from the sense or antisense strand. The design of bisulfite PCR primers was done manually and with the aid from three programs, namely MethPrimer (http://www.urogene.org/methprimer/index1.html), Bisearch (http://bisearch.enzim.hu/), and Primer Express 3.0 (Applied Biosystems).

The final primer sequences were determined after considering following factors:

(i) The forward and reverse primers should have similar melting temperatures to facilitate PCR optimization.

(ii) The primer-dimer and secondary structure of primers should be absent, if possible.

(iii) As the proportion of thymine (T) in the genome increases greatly after bisulfite conversion and may result in many continuous T, the chances of non-specific annealing and amplification of non-specific products are enhanced. Therefore, the primers was checked by the ePCR program in Bisearch to see if there is any non-specific products amplified by the primers in the bisulfite converted genome *in silico*.

(iv) CpG sites are avoided in the primer sequences to minimize biases in amplifying methylated or unmethylated DNA.

In this thesis, bisulfite sequencing assays were named by bis-gene name, such as

bis-GSTP1, bis-SOCS1, bis-APC and bis-p16. For the sequencing of internal control amplicons, as the four real-time PCR assays were designed towards the *ACTB* gene and in proximity to each other, therefore, one assay named Actin_GPS was designed to sequence the amplicons β-actin***g**stp1 control, β-actin***p**16 control and β-actin***s**ocs1 control, and another assay named Actin_APC was to sequence the β-actin*apc control.

3.5.4. Conventional PCR after bisulfite treatment

The bisulfite-treated DNA was amplified by conventional PCR using the AmpliTaq Gold polymerase and the GeneAmp PCR Core Reagent Kit (Applied Biosystems) in a total volume of 25 μL for bis-GSTP1, bis-SOCS1, bis-APC, bis-p16 and Actin_APC assays. For the Actin_GPS assay, HotStarTaq DNA Polymerase and the provided reagents (Qiagen, Hilden, Germany) was mixed in a total volume of 10 μL. To the former assays, corresponding primers, 1X PCR Buffer II, 3 mM of $MgCl_2$, 200 μM of dNTP mix (Promega, Madison, WI) and 1.25 U AmpliTaq Gold polymerase were added with 2 μL of bisulfite-treated DNA (except in bis-p16 amplification, 2.5 mM $MgCl_2$ was used). For the Actin_GPS assay, 1X HotStar Buffer and corresponding primers, 1 mM $MgCl_2$, 200 μM of dNTP mix and 0.4 U of HotStarTaq polymerase were mixed with 1 μL bisulfite-treated DNA. The thermal profile for the assay using GeneAmp PCR Core Reagent kit was 95°C for 10 min, followed by denaturation at 95°C for 40 s, annealing at corresponding temperatures, and extension at 72°C for 40 s for 40 cycles and a final incubation at 72°C for 10 min. The thermal profile for the assay using the HotStarTaq polymerase was 94°C for 15 min to activate the polymerase, and followed by denaturation at 94°C for 20 s, annealing at 59°C for 30 s, and extension at 72°C for 1 min for 45 cycles and a final

incubation at 72°C for 3 min.

Table 3.5.1. Primer sequences for conventional PCR for amplifying DNA after bisulfite treatment

Amplicon	Oligonucleotide	Sequence (5' to 3')	Product length (bp)	Annealing temperature (°C)	Remarks
GSTP-1	bis-Gstp1-02F	TTGTTTTGTGAAGYGGGTGTGTAAGTTTYG	363	66	
	bis-Gstp1-02R	ACCTCRCRACCTCCRAACCTTATAAAAATA			
APC	bis-apc-02F	TGTTTGTTGGGGATTGGGGT	323	62	
	bis-apc-02R	AACCTAACCATAATAACTCCAACACCTACC			
SOCS-1	bis-socs1-02F	GGTTTYGGTTTTYGGYGATAYGTATTTT	329	65	
	bis-socs1-02R	AATYGAAACTCTYGYGACTACCATCCA			
p16	bis_newp16_469F	GAGGGGTTGGTTGGTTATTAGA	262	62	2.5 mM $MgCl_2$ was used
	bis_newp16_730R	TACAAACCCTCTACCCACCTAAA			
Actin_APC	bis_act_apc_15F	GATTAGTGTTTGTTTTTTATGGTAATAA	451	60	
	bis_act_apc_465R	TTCTAACCCATACCCACCAT			
Actin_GPS	bis_act_gps_142F	AGGGGGTAAAAAAATGTTGTATT	512	59	HotStarTaq polymerase was used
	bis_act_gps_653R	ATTAACAAAAACCCRACTCAAACA			

Notes
Bis: primer in bisulfite assays
F: Forward primer
R: Reverse primer
Act: primer in *ACTB* amplicon

Table 3.5.2. PCR reaction conditions and thermal profiles for conventional PCRs for (A) bis-GSTP1,bis-SOCS1, bis-APC , Actin_APC , (B) bis-p16 and (C) Actin_GPS

Assay conditions	**(A)**	**(B)**
10X PCR Buffer II	1X	1X
$MgCl_2$ (25mM)	3 mM	2.5 mM
dNTP (2.5mM)	200 µM	200 µM
Forward primer(10µM)	200 µM	200 µM
Reverse primer(10µM)	200 µM	200 µM
AmpliTaq Gold	1.25 U	1.25 U
Bisulfite converted DNA	2 µL	2 µL
Total	25 µL	25 µL

PCR profile (A,B)			
Activation of AmpliTaq Gold polymerase	95°C	10 min	
Denaturation	95°C	40 s	40 cycles
Annealing	assay-dependent	1 min	
Extension	72°C	40 s	
Final extension	72°C	7 min	

Assay conditions	**(C)**
10X HotStar Buffer*	1X
$MgCl_2$ (25mM)	1 mM
dNTP (2.5mM)	200 µM
Forward primer (10µM)	200 µM
Reverse primer (10µM)	200 µM
HotStar Taq	0.4 U
Bisulfite converted DNA	1 µL
Total	10 µL

*Already contain 1.5 mM $MgCl_2$

PCR profile (C)			
Activation of HotStarTaq polymerase	94°C	15 min	
Denaturation	94°C	20 s	45 cycles
Annealing	59°C	30 s	
Extension	72°C	1 min	
Final extension	72°C	3 min	

3.5.5. Cloning and bisulfite genomic sequencing

After PCR amplification, the products were cloned for subsequent sequencing using the pGEM®-T Easy Vector System (Promega, Madison, WI). The ligation was done by mixing 1X Rapid Ligation Buffer, 50 ng pGEM®-T Easy Vector, 3 Weiss units of T4 DNA Ligase and 3 μL PCR products and incubated at 16°C overnight. As the AmpliTaq Gold polymerase and the HotStarTaq polymerase generate an extra A-overhang in PCR products during PCR, the vector has a 3'T-overhang to provide a compatible end for ligation and also prevent the vector to re-circularize.

The transformation was started by incubating 10 μL of ligation products with 60 μL of the *Escherichia coli* strain JM109 High Efficiency Competent Cells (Promega) on ice for 30 min. Heat-shock was performed at 42°C for 1 min followed by 2 min chilling on ice. 260 μL SOC (Super Optimal broth with Catabolite repression) medium (Invitrogen, Carlsbad, CA) was added to recover the cells. The cells were incubated at 37°C for 1.5 hr with shaking. As the cloning site of the pGEM®-T Easy Vector is within the α-peptide coding region of the enzyme β-galactosidase, this allows blue-white screening to pick up the recombinant clones later on. After the cells were centrifuged at 1,000 *g* for 10 min and resuspended in 100 μL SOC Medium, 40 μL X-Gal and 20 μL IPTG were added to each sample and plated onto LB/ampicillin plates. The plates were incubated overnight at 37°C.

Sixteen white recombinant colonies were picked from each sample plate into 10 μL deionized water and lysed at 95°C for 3 min. The plates were stored at 4°C for later use, if needed. Then a colony PCR using the SP6 and T7 RNA polymerase promoters as primers was performed. The sequences of SP6 and T7 primers are

5'-ATT TAG GTG ACA CTA TAG AA-3' and 5'-TAA TAC GAC TCA CTA TAG GG-3' (Proligo). In a total volume of 12.5 µL, 1X Buffer II, 2.5 mM $MgCl_2$, 200 µM dNTP mix, 100 nM of SP6 and T7 primers and 1.25 U of AmpliTaq Gold polymerase were added with 1.5 µL colony DNA template solution. The PCR was started at 95°C for 10 min, followed by denaturation at 95°C for 40 s, annealing at 55°C for 1 min and extension at 72°C for 40 s for 30 cycles and a final incubation at 72°C for 7 min.

Gel electrophoresis was run to confirm the presence of insert by checking the size of DNA band. Cycle sequencing reaction was performed afterwards using BigDye Terminator Cycle Sequencing version 1.1 Kit (Applied Biosystems). In a 10 µL reaction, 2 µL Ready Reaction Premix, 1X BigDye Sequencing Buffer, 160 nM sequencing primer (SP6 primer) and 1 µL template of the cloned PCR product were mixed together. The thermal profile was 96°C for 30 s, 50°C for 15 s and 60°C for 4 min for 25 cycles. The products were precipitated by ethanol/sodium acetate method and denatured with 10 µL of HiDi Formamide (Applied Biosystems) at 95°C for 3 min. Samples were then sequenced using the ABI PRISM® 3100 Genetic Analyzer (Applied Biosystems).

3.5.6. Data acquisition and interpretation

The fluorescence data were collected and interpreted by the ABI PRISM® 3100 Genetic Analyzer Data Collection Software v1.0.1 which displayed the data as an electropherogram. The sequences were analyzed by aligning to the template sequences using the Seqscape Software and the methylation status of CpG sites were scored manually. Eight clones were selected from each sample according to their

sequencing quality determined by the Seqscape Software and the completeness of alignment to the target amplicons. As mentioned in Chapter 3.5.1, after bisulfite conversion, unmethylated cytosine would change to thymine while methylated cytosine would remain as cytosine. The methylation status of all clones from sequencing was illustrated as dot diagrams. A closed circle represented a methylated cytosine in a CpG site and an open circle represented an unmethylated cytosine in a CpG site. Details are discussed in Chapter 4.2.

SECTION III: DEVELOPMENT OF METHYLATION MARKERS IN HCC DETECTION

Chapter 4: Evaluation of the real-time PCR assay for quantification of methylated tumor suppressor genes

4.1. Development of real-time PCR assays

The quantification of tumor suppressor genes was performed by a duplex real-time PCR system described in chapter 3. The use of a standard curve in real-time PCR allowed the absolute quantification of nucleic acids by amplifying the serially diluted calibrators derived from buffy coat DNA from normal individuals. The calibration curves were designed to amplify specifically for the sequences of *GSTP1, SOCS1, APC* and *p16* and their corresponding *ACTB* regions in each assay. The concentrations of the calibrators were from 10,000 copies to 2.4 copies, in all amplification systems. For the *GSTP1* calibration curve, the slope was -3.64 and correlation coefficient (R^2) was 0.997. For the *SOCS1* calibration curve, the slope was -3.81 and correlation coefficient (R^2) was 0.990. For the *APC* calibration curve, the slope was -3.94 and correlation coefficient (R^2) was 0.997. Finally, for the *p16* calibration curve, the slope was -3.74 and correlation coefficient (R^2) was 0.991 (Table 4.1.1). As mentioned in Chapter 3, an internal control system amplifying a region in the *ACTB* gene (specifically designed for each amplicon) was also co-amplified in the real-time PCR of each TSG to indicate the completeness of enzyme digestion. For the internal control for *GSTP1* (β-actin*gstp1 control), the slope of calibration curve was -3.66 and the correlation coefficient (R^2) was 0.986. And for the internal control for *SOCS1* (β-actin*socs1 control), the slope of

calibration curve was -4.68 and the correlation coefficient (R^2) was 0.907. For the internal control of *APC* (β-actin*apc control), the slope of calibration curve was -3.73 and the correlation coefficient (R^2) was 0.987. Finally, for the *p16* (β-actin*p16 control), the slope of calibration curve was -4.23 and the correlation coefficient (R^2) was 0.975 (Table 4.1.1 and Figure 4.1.1). The PCR efficiencies of the standard curve in duplex real-time PCR had been optimized as high as possible. The PCR efficiencies of the amplification of target genes ranged from 79.4% to 88.2% and the PCR efficiencies of the amplification of internal control ranged from 63.6% to 87.6%.

Table 4.1.1. The slope, PCR efficiency and correlation coefficient of the calibration curves in real-time PCR assays

Assay	Slope	PCR efficiency	Correlation coefficient (R^2)
GSTP1	-3.64	88.2%	0.997
β-actin*gstp1 control	-3.66	87.6%	0.986
SOCS1	-3.81	83.0%	0.990
β-actin*socs1 control	-4.68	63.6%	0.907
APC	-3.94	79.4%	0.997
β-actin*apc control	-3.73	85.4%	0.987
p16	-3.74	85.1%	0.991
β-actin*p16 control	-4.23	72.3%	0.975

(A) The real-time PCR calibration curves for *GSTP1* (left) and its internal control (β-actin*gstp1 control) (right)

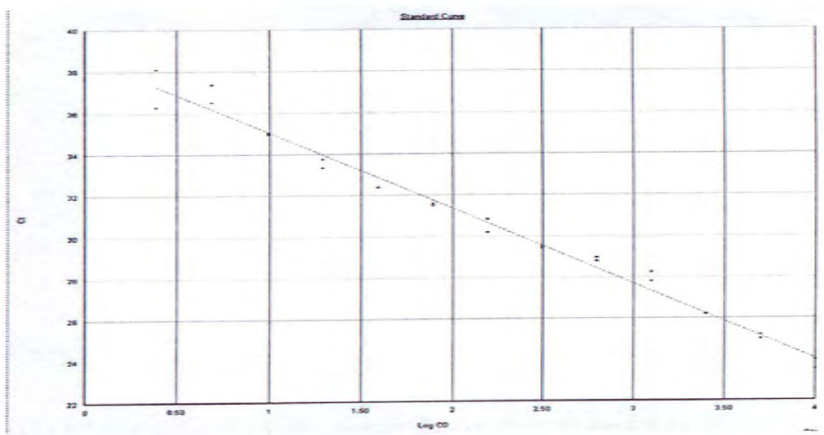

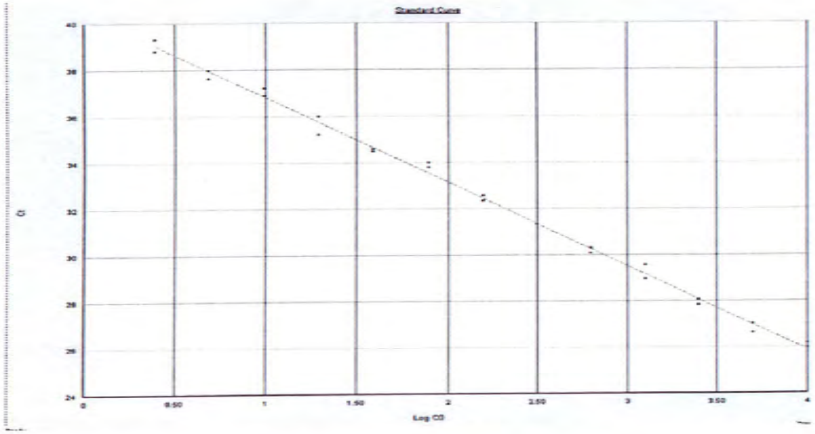

(B) The real-time PCR calibration curves for *SOCS1* (left) and its internal control (β-actin*socs1 control) (right)

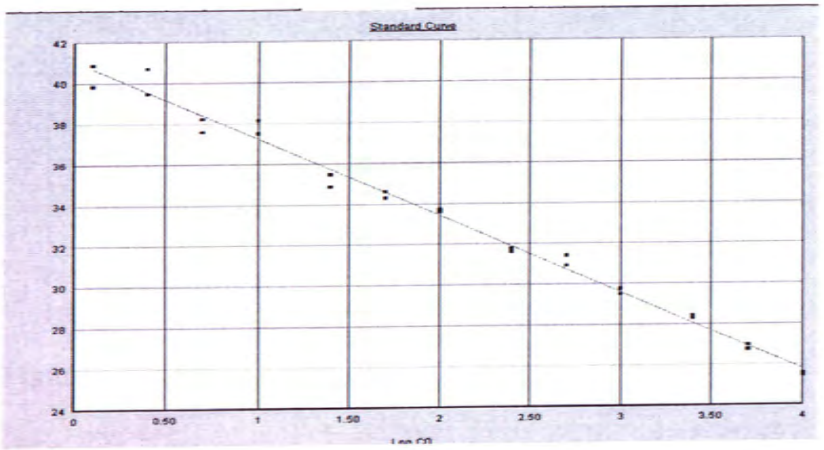

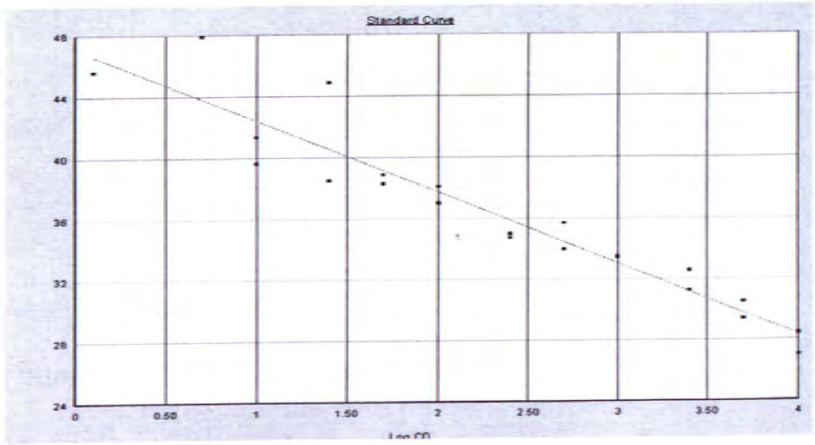

(C) The real-time PCR calibration curves for *APC1* (left) and its internal control (β-actin*apc control) (right)

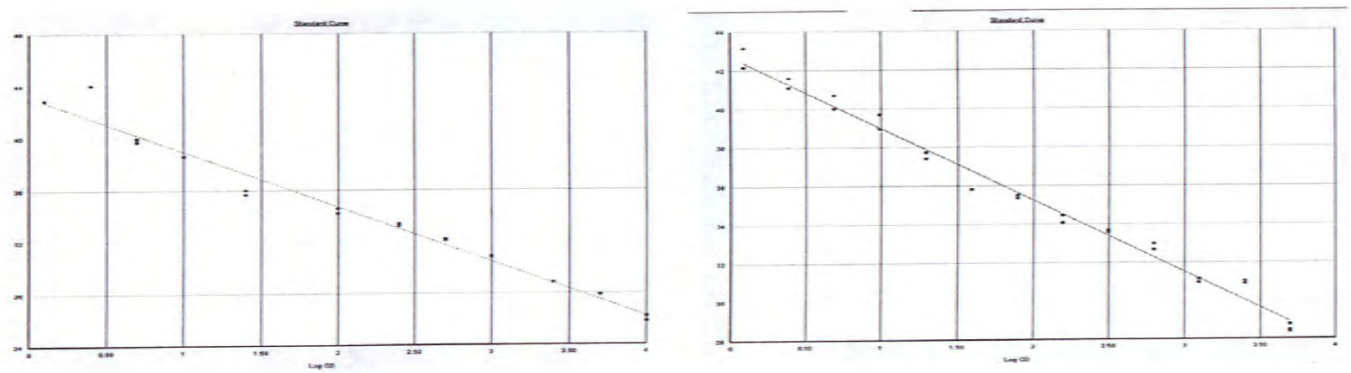

(D) The real-time PCR calibration curves for *p16* (left) and its internal control (β-actin*p16 control) (right)

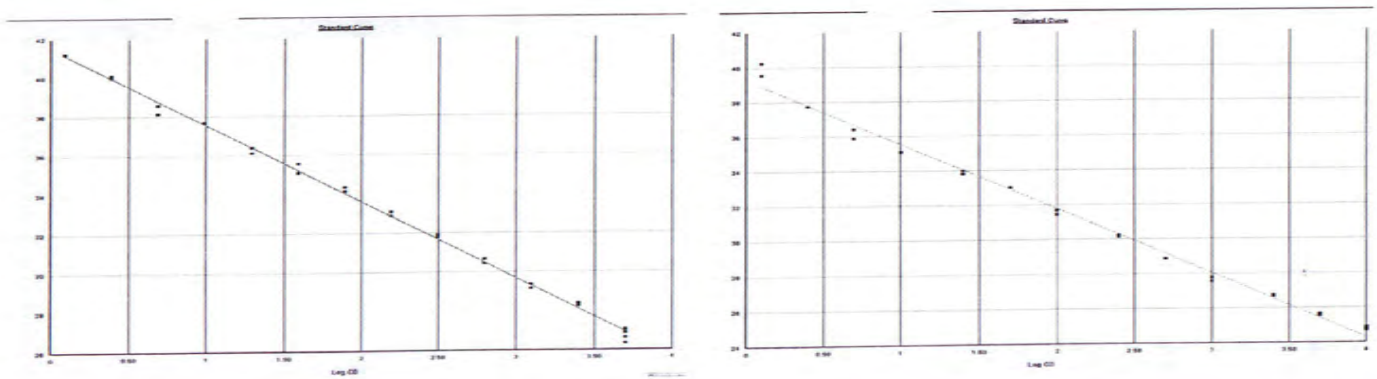

Figure 4.1.1. The standard curves for the real-time PCRs of the tumor suppressor genes quantification assays

4.2. Methylation analyses by bisulfite sequencing were concordant with the real-time quantification results

Methylation patterns of the *GSTP1*, *SOCS1*, *APC*, *p16* and *ACTB* genes in paired HCC tissue and blood cells were analyzed by bisulfite sequencing (Frommer *et al*, 1992), to determine whether the real-time quantification assays were reflecting the methylation status in the tumor tissue and blood cells. Five pairs of tumor tissues and blood cells from HCC patients were studied. The methylation status of all clones determined by sequencing are illustrated as dot diagrams. Each row represents one DNA molecule and a total of eight clones were analyzed for each sample. The top row of a dot diagram represented the relative nucleotide position of the CpG sites to the transcriptional start site (+1). Negative numbers indicate locations upstream from the transcriptional start site. The data of one representative paired sample of tumor tissue and blood cells for each assay were shown in Figure 4.2.1.

Among the five cases analyzed by bisulfite sequencing analysis, methylated *GSTP1* sequences can be observed in all of the tumor tissues while most of CpG sites in blood cells were unmethylated. The corresponding *ACTB* sequences were unmethylated in both the tumor tissues and blood cells. The real-time analyses of the tumoral and blood cell DNA after restriction enzyme digestion showed concordant results with those using bisulfite sequencing analysis. *GSTP1* sequences were detectable in all of the tumor tissue DNA but none of the blood cell DNA whereas *ACTB* sequences were not detectable in any of the digested tumor tissues nor blood cell DNA.

In the bisulfite sequencing analysis for *SOCS1*, two out of five tumor tissues were hypermethylated while most of CpG sites in blood cells were unmethylated. Almost all of the CpG sites in the corresponding *ACTB* were unmethylated except one. The real-time analysis of the tumor and blood cell DNA after restriction enzyme digestion showed concordant results with bisulfite sequencing. After enzyme digestion, *SOCS1* sequences were detectable in tumor tissues with aberrant methylation status and undetectable in tumor tissues without aberrant DNA methylation whereas none of the blood cells samples had detectable *SOCS1* signal. The corresponding *ACTB* sequences were detectable in neither tumor tissue DNA nor blood cell DNA.

In the bisulfite sequencing analysis for *APC*, four out of five tumor tissues were hypermethylated while none of the blood cells had methylated CpG sites. Almost all of the CpG sites in the corresponding *ACTB* were unmethylated except that some samples had one to two methylated CpG sites. Real-time analyses of the tumor tissues and blood cells DNA after restriction enzyme digestion showed concordant results with bisulfite sequencing. After enzyme digestion, *APC* sequences were only detectable in tumor tissues with aberrant methylation status whereas *APC* sequences were not detected in any blood cell DNA samples. The corresponding *ACTB* sequences were not detectable in any tumor tissue nor blood cell DNA.

For the *p16* bisulfite sequencing analysis, two out of five tumor tissues were hypermethylated. On the other hand, the DNA samples from blood cells were generally unmethylated. The CpG sites in the corresponding *ACTB* region were generally unmethylated except the last CpG site (+340) was occasionally methylated.

On the other hand, the real-time analyses of the tumor and blood cell DNA after restriction enzyme digestion showed concordant results with bisulfite sequencing. After enzyme digestion, *p16* sequences were only detectable in tumor tissues with aberrant DNA methylation whereas *p16* sequences were not detected in any of the blood cells samples. The corresponding *ACTB* sequences were not detectable in any of the tumor tissues and blood cell DNA samples.

(A) GSTP1 and *ACTB* (*GSTP1* control)

GSTP1

Sample	CpG sites																		
	-331	-310	-308	-300	-297	-295	-287	-282	-273	-268	-231	-197	-187	-185	-182	-176
Tumour tissue #15	○	○	●	○	○	○	○	●	○	○	○	○	○	○	○	○
	○	○	○	○	●	●	●	○	○	○	○	●	●	●	●	○
	○	●	●	○	●	●	●	○	○	○	●	●	●	●	●	●
	○	●	●	●	●	○	●	●	●	●	●	●	●	●	●	●
	●	●	●	●	●	●	●	○	●	●	●	●	●	●	●	●
Blood cells #15	○	○	○	○	○	○	○	○	○	○	○	○	○	○	○	○
	○	○	○	○	○	○	○	○	○	○	○	○	○	○	○	○
	○	○	○	○	○	○	○	○	○	○	○	○	○	○	○	○
	○	○	○	○	○	○	○	○	○	○	○	○	○	○	○	○
	○	○	○	○	○	○	○	○	○	○	○	○	○	○	○	○

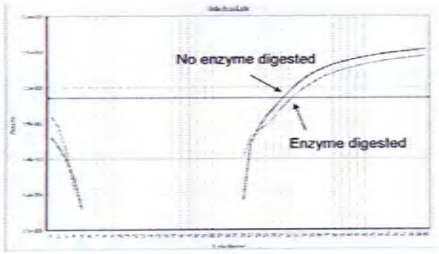

ACTB
(GSTP1 control)

Sample	CpG sites																								
	-90	-87	-82	-61	-57	-53	-51	-48	-45	-28	-25	-23	-20	-18	-9	-6	1	3	7	12	14	28	37	42	45
Tumour tissue #15	○	○	○	○	○	○	○	○	○	○	○	○	○	○	○	○	○	○	○	○	○	○	○	○	○
	○	○	○	○	○	○	○	○	○	○	○	○	○	○	○	○	○	○	○	○	○	○	○	○	○
	○	○	○	○	○	○	○	○	○	○	○	○	○	○	○	○	○	○	○	○	○	○	○	○	○
	○	○	○	○	○	○	○	○	○	○	○	○	○	○	○	○	○	○	○	○	○	○	○	○	○
	○	○	○	○	○	○	○	○	○	○	○	○	○	○	○	○	○	○	○	○	○	○	○	○	○
Blood cells #15	○	○	○	○	○	○	○	○	○	○	○	○	○	○	○	○	○	○	○	○	○	○	○	○	○
	○	○	○	○	○	○	○	○	○	○	○	○	○	○	○	○	○	○	○	○	○	○	○	○	○
	○	○	○	○	○	○	○	○	○	○	○	○	○	○	○	○	○	○	○	○	○	○	○	○	○
	○	○	○	○	○	○	○	○	○	○	○	○	○	○	○	○	○	○	○	○	○	○	○	○	○
	○	○	○	○	○	○	○	○	○	○	○	○	○	○	○	○	○	○	○	○	○	○	○	○	○

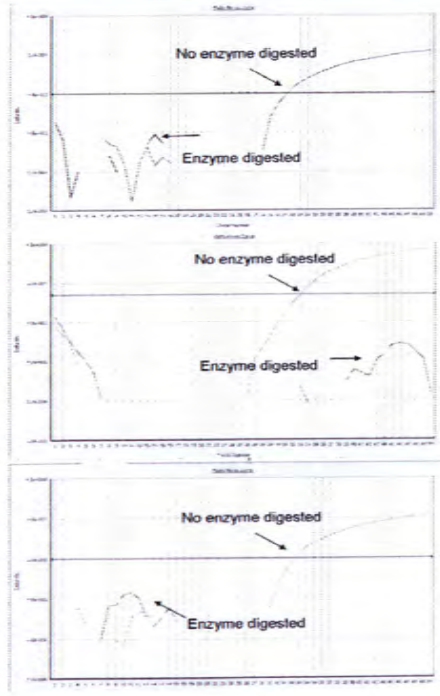

(B) *SOCS1* and *ACTB* (*SOCS1* control)

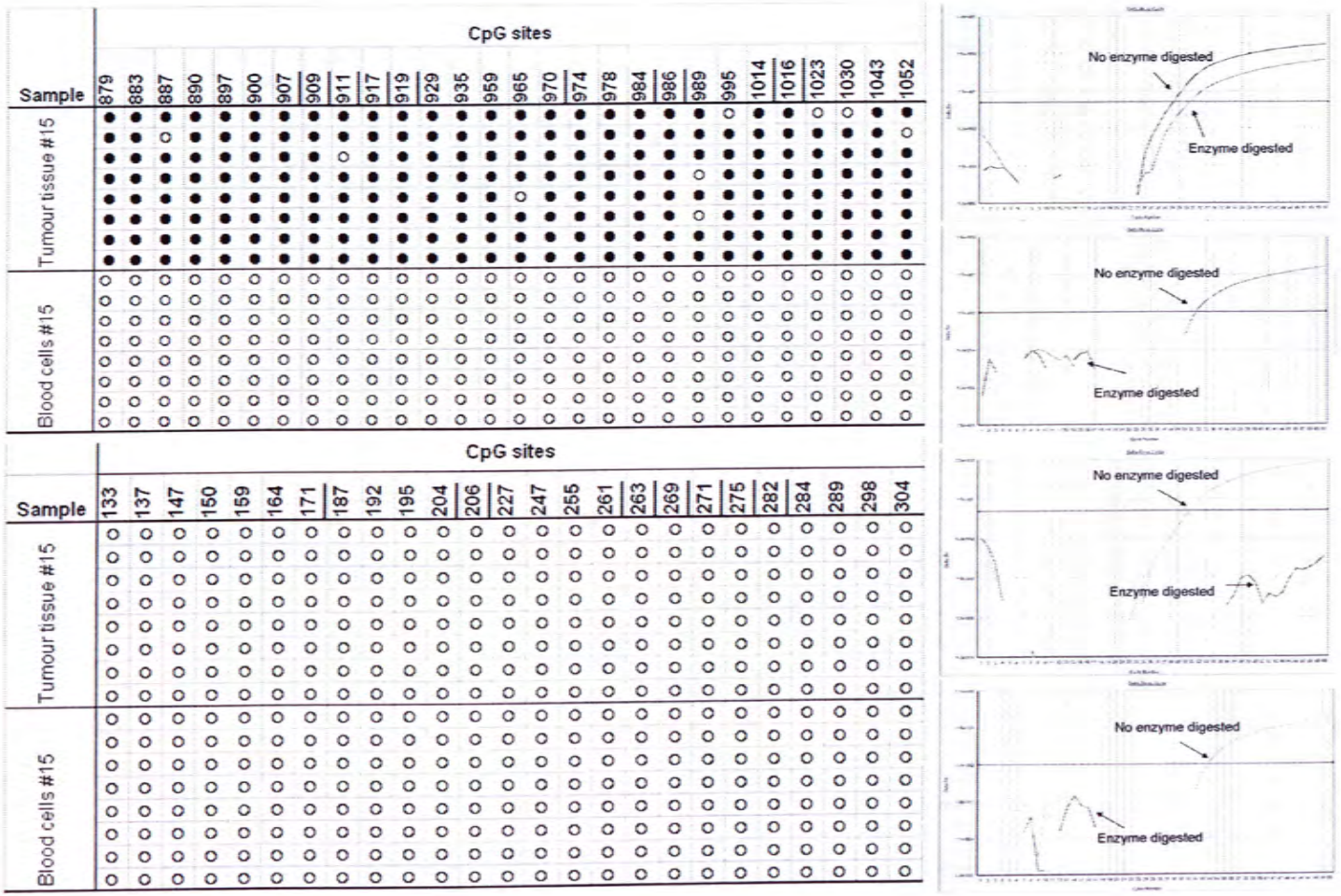

(C) *APC* and *ACTB* (*APC* control)

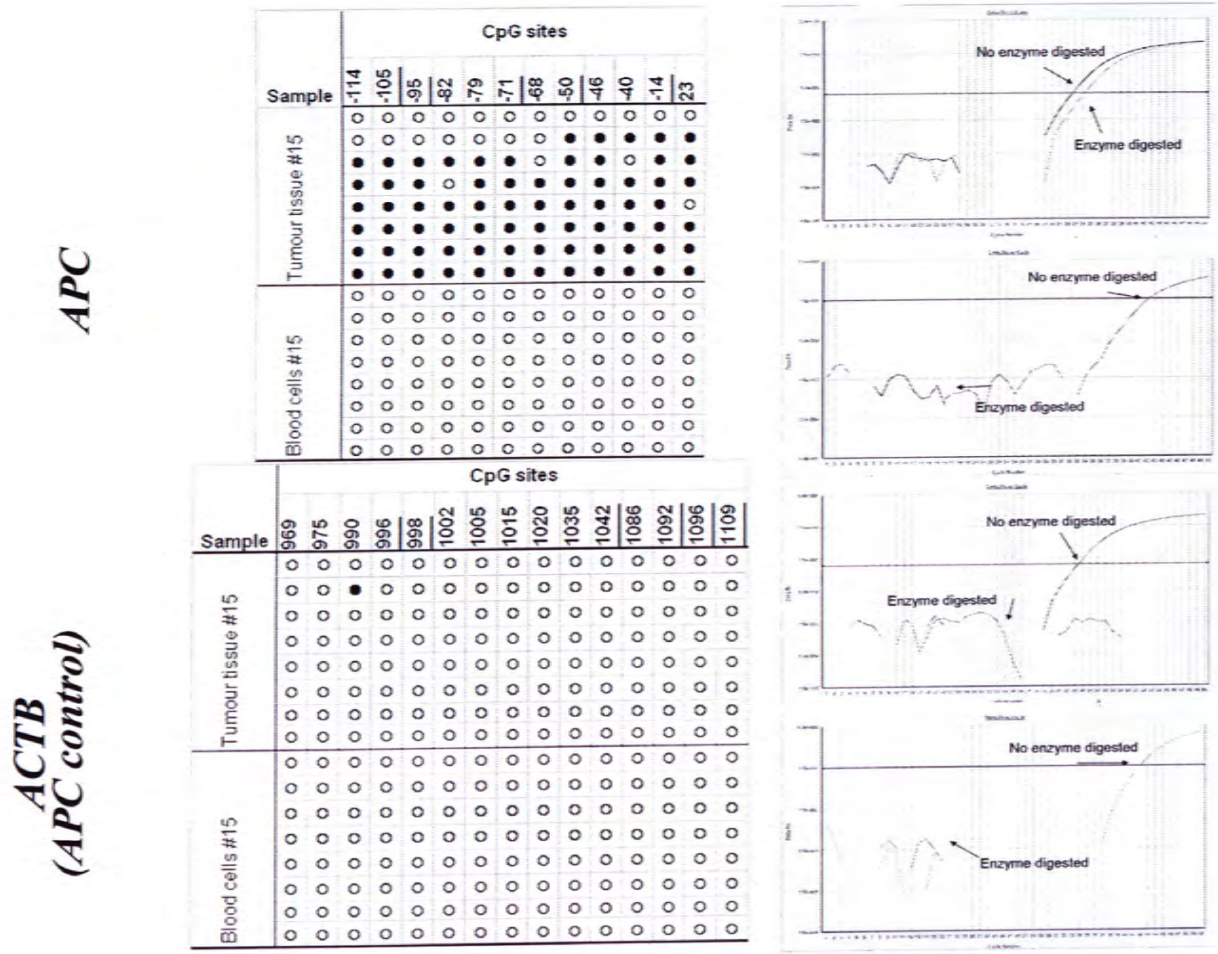

(D) *p16* and *ACTB* (*p16* control)

P16

Sample	CpG sites												
	149	154	156	160	164	167	173	195	199	202	220		
Tumour tissue #15	○	○	○	○	○	○	○	○	○	○	○		
	○	○	○	○	○	○	○	○	○	○	○		
	○	○	○	○	○	○	○	○	○	○	○		
	○	○	○	○	○	○	○	○	○	○	●		
	●	●	●	●	●	●	●	●	●	●	○		
	●	●	●	●	●	●	●	●	●	●	●		
Blood cells #15	○	○	○	○	○	○	○	○	○	○	○		
	○	○	○	○	○	○	○	○	○	○	○		
	○	○	○	○	○	○	○	○	○	○	○		
	○	○	○	○	○	○	○	○	○	○	○		
	○	○	○	○	○	○	●	○	○	○	○		

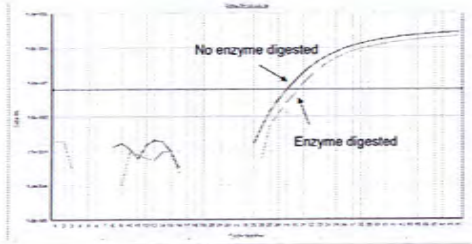

ACTB (p16 control)

Sample	CpG sites															
	247	255	261	263	269	271	275	282	284	289	298	304	309	319	322	340
Tumour tissue #15	○	○	○	○	○	○	○	○	○	○	○	○	○	○	○	●
	○	○	○	○	○	○	○	○	○	○	○	○	○	○	○	●
	○	○	○	○	○	○	○	○	○	○	○	○	○	○	○	●
	○	○	○	○	○	○	○	○	○	○	○	○	○	○	○	●
	○	○	○	○	○	○	○	○	○	○	○	○	○	○	○	●
	○	○	○	○	○	○	○	○	○	○	○	○	○	○	○	●
Blood cells #15	○	○	○	○	○	○	○	○	○	○	○	○	○	○	○	○
	○	○	○	○	○	○	○	○	○	○	○	○	○	○	○	○
	○	○	○	○	○	○	○	○	○	○	○	○	○	○	○	○
	○	○	○	○	○	○	○	○	○	○	○	○	○	○	○	○
	○	○	○	○	○	○	○	○	○	○	○	○	○	○	○	○

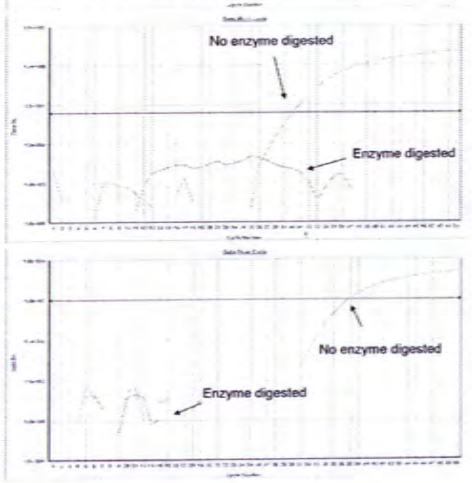

Figure 4.2.1. Bisulfite sequencing data (left, dot diagrams) and the corresponding real-time analysis (right, amplification plots) for the tumor tissue and blood cell DNA of one representative patient

Left: Bisulfite sequencing data of one representative sample of tumor tissue and blood cell DNA for the (A) *GSTP1*, (B) *SOCS1*, (C) *APC* and (D) *p16* genes and the corresponding regions at the *ACTB* gene. The upper panel shows the methylation pattern of TSGs in tumor tissue and blood cell DNA of one HCC patient. The lower panel shows the methylation pattern of the corresponding control in tumor tissue and blood cell DNA of that HCC patient. The top row of the dot diagram represents the relative nucleotide position of the CpG sites in relation to the transcriptional start site (start codon as +1). Negative number indicates an upstream location from exon 1. The underlined CpG site indicates the CpG dinucleotide within the restriction sites involved in the digestion assays. Each row represents one clone and a total of eight clones were analyzed for each sample. Open circles indicates unmethylated CpG sites while filled circles indicate methylated CpG sites.

The amplicons were designed with reference to the *GSTP1* gene (*Homo sapiens*) GenBank Accession NM_000852, the *SOCS1* gene (*Homo sapiens*) GenBank Accession NM_003745, the *APC* gene (*Homo sapiens*) GenBank Accession NM_000038, the *p16* gene (*Homo sapiens*) GenBank Accession NM_000077 and the *ACTB* gene (*Homo sapiens*) GenBank Accession NM_001033084.

The nucleotide positions are numbered according to the start codon of *GSTP1* corresponding to chr11: 67107642; the start codon of *SOCS1* corresponding to chr16: 11255775; the start codon of *APC* corresponding to chr5: 112101455; the start codon of *p16* corresponding to chr9: 21957751 and the start codon of *ACTB* corresponding to chr7: 5533470 of the human genome in the UCSC Genome Browser (hg18, March 2006 assembly).

Right: Real-time analyses of the corresponding samples in bisulfite sequencing.

Chapter 5: Clinical application of methylated markers in the detection of hepatocellular carcinoma

5.1. Demographics of HCC patients and HBV carriers

After evaluating the real-time PCR amplification systems for detecting methylated tumor suppressor genes, samples from HCC patients, HBV carriers and healthy individuals were analyzed to explore the clinical potential of these methylated markers. The HBV carriers had been followed for at least 18 months to confirm that they were free of HCC. Table 5.1.1 shows the demographic information of the HCC patients and HBV carriers. The age of the two groups of subjects were matched within 5 years and there is no statistically significant difference between them (t-test, $P = 0.417$). A male preponderance was shown in both groups with a proportion of male 87.5% and 80% in the HCC patients and in the HBV carriers, respectively (Chi-square test, $P = 0.415$). Ninety-one percent of HCC patients were HBV-infected. None of the HCC patients or the HBV carriers was HCV-infected. The proportions of HBV carriers with cirrhosis were not significantly different between the HCC patients and the HBV carriers. Fifty-five percent of the HCC patients and 9.1% of the HBV carriers had serum AFP level > 20 μg/L and their median serum AFP levels are significantly different (Mann-Whitney test, $p < 0.001$). Table 5.1.2 shows that there are no statistically significant correlations between plasma concentrations of methylated tumor suppressor genes with tumor size except *p16*.

Table 5.1.1. Demographics of the HCC patients and HBV carriers

Variable	HCC patients (n=56)	HBV carriers (n=55)	P-value (univariate)
Age (years)	55.5 (50-63)*	53 (50-59)*	0.417[a]
Sex (% of male)	87.5%	80%	0.415[b]
Hepatitis B infection, n (%)	51 (91)	55 (100)	NA
Hepatitis C infection, n (%)	0 (0)	0 (0)	NA
Ultrasonographic evidence of cirrhosis, n (%)	23 (41.1)	31 (56.4)	0.155[b]
Serum AFP, μg/L	30 (4-159.25)*	4 (2.5-7)*	<0.001[c]

[a] t-test
[b] Chi-square test
[c] Mann-Whitney test
* Data are represented by the median value (interquartile range)
NA: Not applicable

Table 5.1.2. Correlation of plasma concentrations of methylated *GSTP1, SOCS1, APC* and *p16* sequences and tumor size

	P value*
GSTP1	0.162
SOCS1	0.711
APC	0.300
p16	<0.05

*Spearman correlation analysis

5.2. Quantitative analysis of hypermethylated tumor suppressor genes in tumor and plasma samples

Detection of hypermethylated *GSTP1, SOCS1, APC* and *p16* sequences after MSRE digestion for HCC tumor samples

Among the 56 HCC tumor tissues, 44 (78.6%), 36 (64.3%), 49 (87.5%) and 50 (89.3%) of them were methylated for the *GSTP1, SOCS1, APC and p16* genes, respectively (Table 5.2.1). Twenty-eight (50%) of the HCC patients had all 4 TSGs methylated in the tumor tissues, 25% of them had three methylated TSGs in their tumor tissues and 21.4% of them had two methylated TSGs in their tumor tissues. Only one patient had a single TSG methylated in the tumor, and one had all four TSGs completely unmethylated (Table 5.2.2).

Table 5.2.1. Detection rates of methylated TSGs in HCC tumor tissues

Gene	No. of patients (n=56) with methylation in HCC tumor tissues n, (%)
GSTP1	44 (78.6)
SOCS1	36 (64.3)
APC	49 (87.5)
p16	50 (89.3)

Table 5.2.2. Detection rates of multiple methylated TSGs in HCC tumor tissues

No. of methylated markers in tumor tissues	No. of HCC patients (n=56) n, (%)
0	1 (1.8)

1	1 (1.8)
2	12 (21.4)
3	14 (25.0)
4	28 (50.0)

Detection of hypermethylated *GSTP1, SOCS1, APC* and *p16* sequences after MSRE digestion for the plasma samples of the HCC patients, HBV carriers and healthy individuals

I evaluated the detection rate of methylated TSGs in the corresponding plasma samples for patients with such methylated TSGs in tumor tissues. Of the 44 HCC patients with detectable methylated *GSTP1* in tumor tissues, 24 (54.5%) of them showed detectable methylated *GSTP1* sequences in plasma. Of the 36 HCC patients with detectable methylated *SOCS1* in tumor tissues, 20 (55.6%) of them showed detectable methylated *SOCS1* sequences in plasma. Of the 49 HCC patients with detectable methylated *APC* in tumor tissues, 18 (36.7%) of them showed detectable methylated *APC* sequences in plasma. Of the 50 HCC patients with detectable methylated *p16* in tumor tissues, 33 (66%) of them showed detectable methylated *p16* sequences in plasma.

Table 5.2.3. Detection rates of methylated TSGs in the plasma of HCC patients with methylated TSGs in tumor tissues

TSG (n = no. of patients with methylated TSG in tumor tissue)	No. of HCC patients (with methylated TSG in tumor tissue) with methylated DNA in plasma n, (%)
GSTP1 (n=44)	24 (54.5)

SOCS1 (n=36)	20 (55.6)
APC (n=49)	18 (36.7)
p16 (n=50)	33 (66.0)

Methylation of multiple TSGs was also observed in the plasma samples of the HCC patients. Despite the percentage of patients having all 4 methylated markers was only 5.4%, the percentage of patients with 3, 2 or 1 methylated markers in plasma were 25%, 26.8% and 19.6% respectively. In 23.2% patients, no methylated TSG was detected in the plasma.

Table 5.2.4. Detection rates of multiple methylated TSGs in plasma of HCC patients

No. of methylated markers in plasma	No. of HCC patients (n=56) with methylation in plasma n, (%)
0	13 (23.2)
1	11 (19.6)
2	15 (26.8)
3	14 (25.0)
4	3 (5.4)

The overall detection rates of methylated TSGs sequences after enzyme digestion in the plasma of 56 HCC patients at diagnosis were 42.9%, 35.7%, 32.1% and 58.9% for the *GSTP1, SOCS1, APC* and *p16* sequences, respectively. For the HBV carriers, methylated *GSTP1, SOCS1* and *p16* sequences were detected in 3.6%, 3.6% and 9.1%, respectively. Methylated *APC* sequences were not detectable in the plasma samples of any HBV carriers. Only two (3.4%) of the 58 healthy individuals showed

detectable *APC* sequences. *GSTP1, SOCS1* and *p16* sequences were not detectable in any of the plasma samples from healthy individuals after digestions. (Kruskal-Wallis, $P<0.001$)

Table 5.2.5. Detection rates of methylated TSGs in plasma samples of HCC patients, HBV carriers and healthy individuals

Gene	No. of HCC patients (n=56) with methylated DNA in plasma n, (%)	No. of HBV carriers (n=55) with methylated DNA in plasma n, (%)	No. of healthy controls (n=58) with methylated DNA in plasma n, (%)
GSTP1	24 (42.9)	2 (3.6)	0 (0)
SOCS1	20 (35.7)	2 (3.6)	0 (0)
APC	18 (32.1)	0 (0)	2 (3.4)
p16	33 (58.9)	5 (9.1)	0 (0)

Overall, at least one of the four TSG sequences could be detected in the plasma of 76.8% (43 of 56) of HCC patients, 14.5% (8 of 55) of HBV carriers and 3.4% (2 of 58) of healthy individuals.

Table 5.2.6. Detection rates of at least one hypermethylated TSG marker in the plasma of HCC patients, HBV carriers and healthy individuals

No. of HCC patients (n=56) with at least one methylated TSGs detected in plasma n, (%)	No. of HBV carriers (n=55) with at least one methylated TSGs detected in plasma n, (%)	No. of healthy controls (n=58) with at least one methylated TSGs detected plasma n, (%)
43 (76.8)	8 (14.5)	2 (3.4)

(A) *GSTP1*

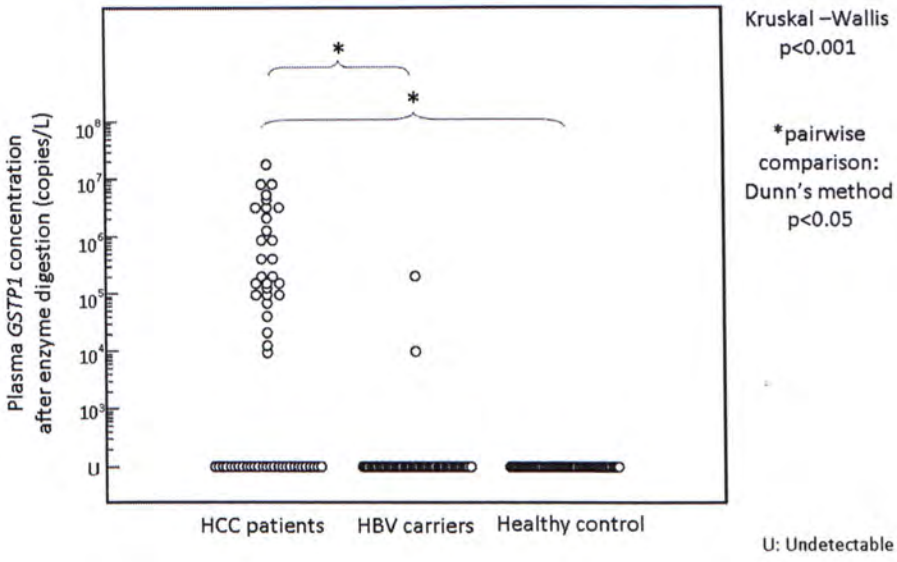

(B) *SOCS1*

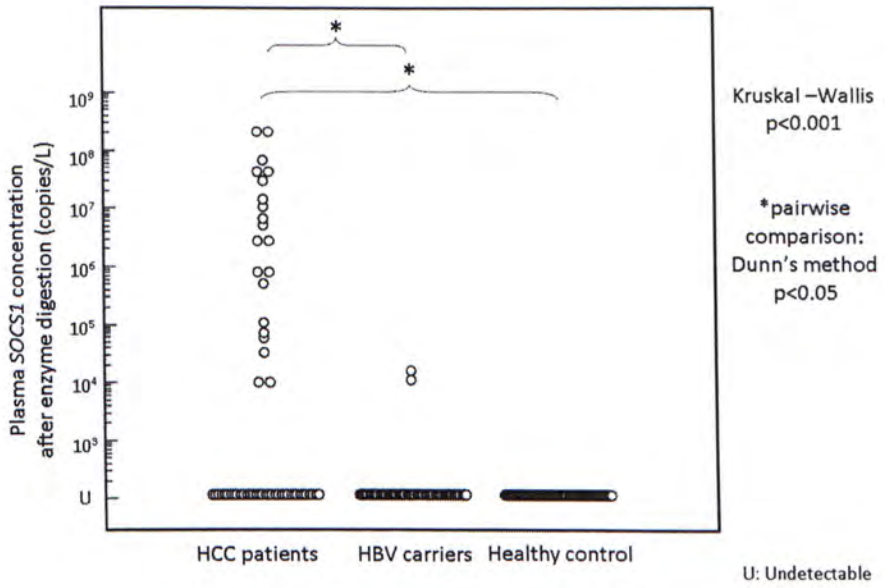

(C) *APC*

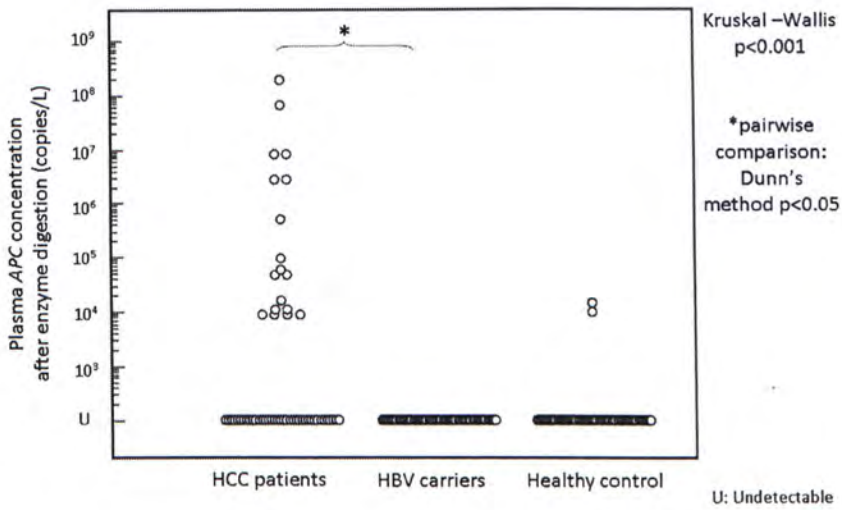

(D) *p16*

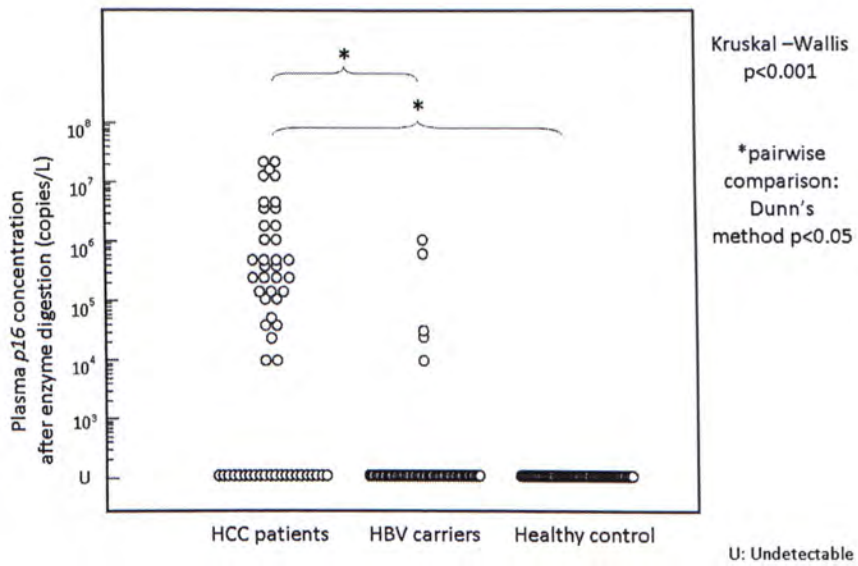

Figure 5.2.1. Plasma concentrations of methylated *GSTP1 (A), SOCS1 (B), APC (C)* and *p16 (D)* sequences after enzyme digestion in the plasma of 56 HCC patients, 55 HBV carriers and 58 healthy individuals

5.3. Effect of cirrhosis on the plasma methylated tumor suppressor gene concentrations

For both of the HCC patients and HBV carriers, subjects with and without ultrasonographic evidence of cirrhosis did not have significant difference in the plasma concentrations of each of the four methylated TSGs.

For the HCC patients with cirrhosis, 12 of the 23 patients had detectable *GSTP1* sequence in their plasma, whereas 16 of the 33 HCC patients without cirrhosis had detectable *GSTP1* sequences in their plasma. The proportion of methylated *GSTP1* in plasma of HCC patients with and without ultrasonographic evidence of cirrhosis was not statistically different (Mann-Whitney test, P = 0.650). For the HBV carriers with cirrhosis, 2 of the 31 subjects had detectable *GSTP1* sequences in their plasma whereas none of the 24 HBV carriers without cirrhosis had detectable *GSTP1* sequences in their plasma. The proportion of methylated *GSTP1* in the plasma of HBV patients with and without ultrasonographic evidence of cirrhosis was not statistically significantly different (Mann-Whitney test P = 0.219).

For the HCC patients with cirrhosis, 8 of the 23 patients had detectable *SOCS1* sequences in their plasma whereas 12 of the 33 HCC patients without cirrhosis had detectable *SOCS1* sequences in their plasma. The proportion of methylated *SOCS1* in plasma of HCC patients with and without ultrasonographic evidence of cirrhosis was not statistically significantly different (Mann-Whitney test, P = 0.863). For the HBV carriers with cirrhosis, 1 of the 31 subjects with detectable *SOCS1* sequences in the plasma whereas 1 of the 24 HBV carriers without cirrhosis had detectable

SOCS1 sequences in the plasma. The proportion of methylated *SOCS1* sequences in plasma of HBV patients with and without ultrasonographic evidence of cirrhosis was not statistically significantly different (P = 0.896, Mann-Whitney test).

For the HCC patients with cirrhosis, 8 of the 23 patients had detectable *APC* sequences in their plasma whereas 10 of the 33 HCC patients without cirrhosis had detectable *APC* sequences in their plasma. The proportion of methylated *APC* in plasma of HCC patients with and without ultrasonographic evidence of cirrhosis was not statistically significantly different (Mann-Whitney test, P = 0.786). For HBV carriers with cirrhosis, none of the 31 patients had detectable *APC* sequences in their plasma whereas none of the 24 HBV carriers without cirrhosis had detectable *APC* sequences in their plasma. The proportion of methylated *APC* in plasma of HBV patients with and without ultrasonographic evidence of cirrhosis was not statistically different (Mann-Whitney test, P = 1.000).

For the HCC patients with cirrhosis, 12 of the 23 patients had detectable *p16* sequence in their plasma, while for HCC patients without cirrhosis, 22 of the 33 patients had detectable *p16* sequences in their plasma. The proportion of methylated *p16* in plasma of HCC patients with and without ultrasonographic evidence of cirrhosis was not statistically significantly different (Mann-Whitney test, P = 0.201). For HBV carriers with cirrhosis, 3 of the 31 patients had detectable *p16* sequences in their plasma whereas 2 of the 24 HBV carriers without cirrhosis had detectable *p16* sequences in their plasma. The proportion of methylated *p16* in plasma of HBV patients with and without ultrasonographic evidence of cirrhosis was not statistically significantly different (Mann-Whitney test, P = 0.878).

(A) *GSTP1*

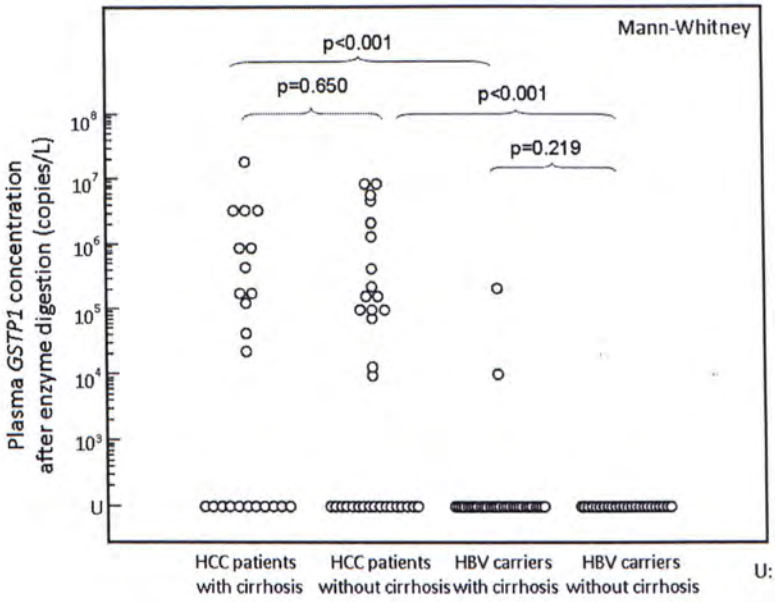

(B) *SOCS1*

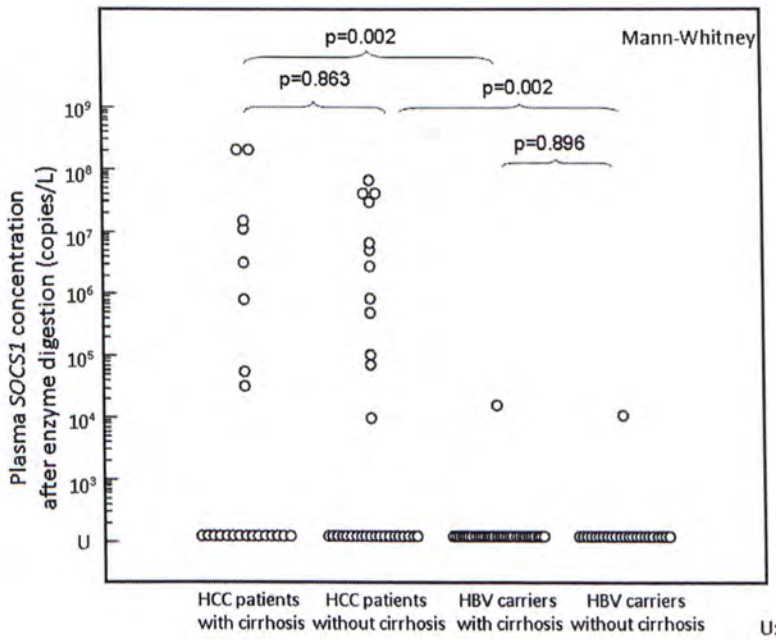

(C)*APC*

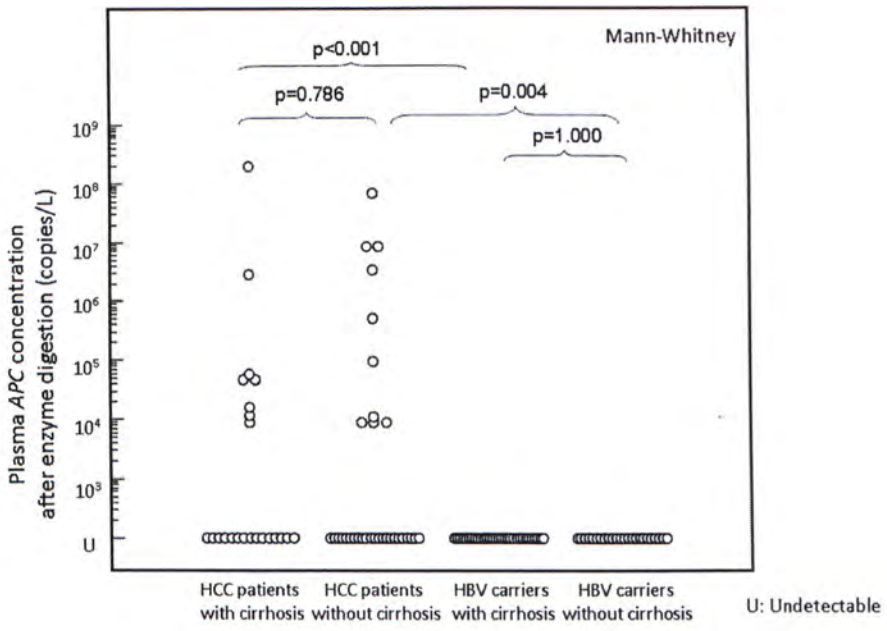

(D) *p16*

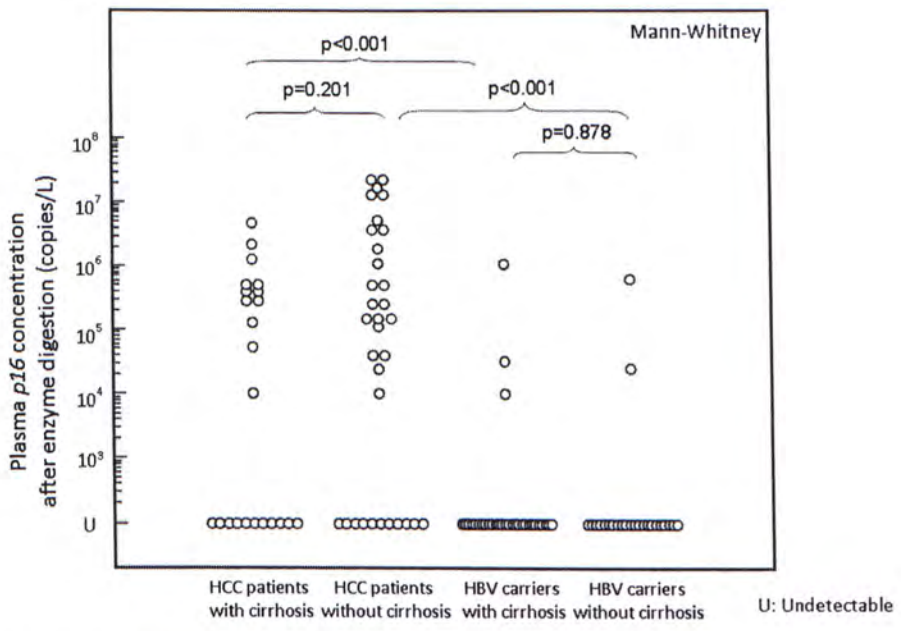

Figure 5.3.1. Plasma concentrations of methylated *GSTP1 (A), SOCS1 (B), APC (C)* and *p16 (D)* sequences after enzyme digestion in the plasma of 56 HCC patients and 55 HBV carriers with and without cirrhosis

5.4. Changes in the concentration of the tumor suppressor genes one month after surgical resection of the cancer

Postoperative blood samples from 34 HCC patients were collected at one month after surgical resection of the liver. The concentrations of methylated TSGs in postoperative samples were compared to those of the preoperative samples. A general decrease in the concentration was observed for the four TSGs. The numbers of patients with detectable *GSTP1, SOCS1, APC* and *p16* sequences at diagnosis were 16, 15, 14 and 22, respectively, and 93.8%, 80%, 92.9% and 86.4% of these patients showed reduced concentrations at one month after surgery. The patients with undetectable TSGs sequences at diagnosis also showed undetectable levels at one month after surgery. The median concentration of methylated *GSTP1* sequences decreased from 5.95×10^5 copies/L to 0 copy/L (Wilcoxon test, $P<0.001$). The median concentration of methylated *SOCS1* sequences decreased from 2.50×10^6 copies/L to 0 copy/L (Wilcoxon test, $P = 0.018$). The median concentration of methylated *APC* sequences decreased from 6.87×10^4 copies/L to 1.01×10^4 copies/L (Wilcoxon test, $P = 0.007$) . The median concentration of methylated *p16* sequences decreased from 3.22×10^5 copies/L to 2.36×10^4 copies/L (Wilcoxon test, $P = 0.006$).

One sample showed an increase in concentration of *p16* from 1.20×10^7 copies/L to 3.07×10^7 copies/L (2.5 fold) at one month after liver resection. Although this trend could not be observed in other TSG sequences, this sample showed high levels in both of the preoperative and the postoperative plasma of *GSTP1* and *APC* (*GSTP1* 7.51×10^6 copies/L and 2.30×10^6 copies/L, respectively, and *APC* with 8.44×10^6 copies/L to 2.26×10^6 copies/L). No *SOCS1* sequences were present in the

preoperative and postoperative plasma samples.

(A) *GSTP1*

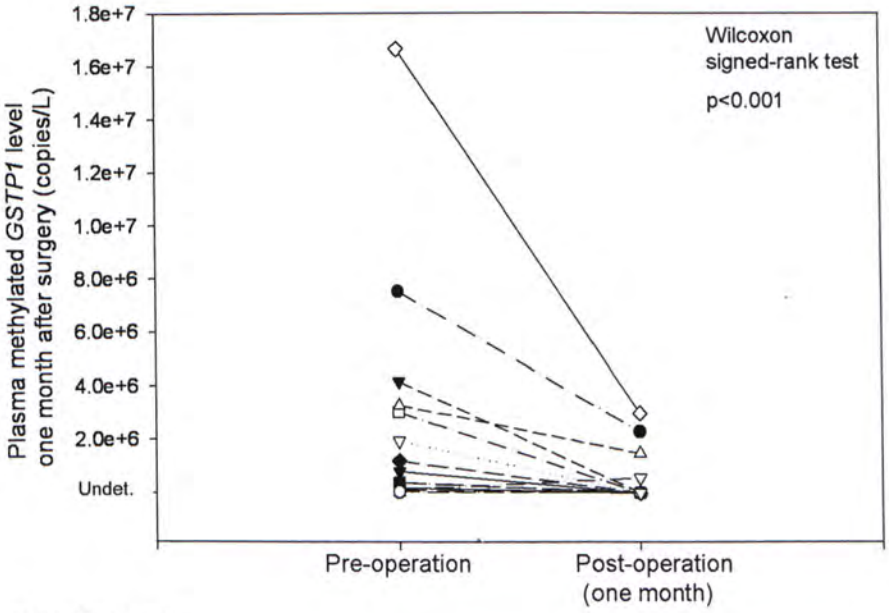

Undet.: Undetectable

(B) *SOCS1*

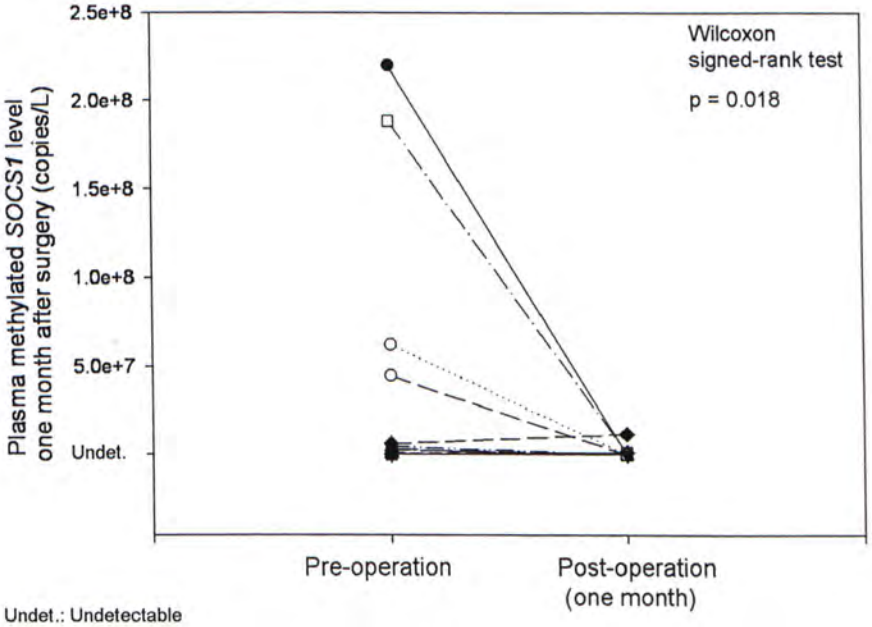

Undet.: Undetectable

(C) *APC*

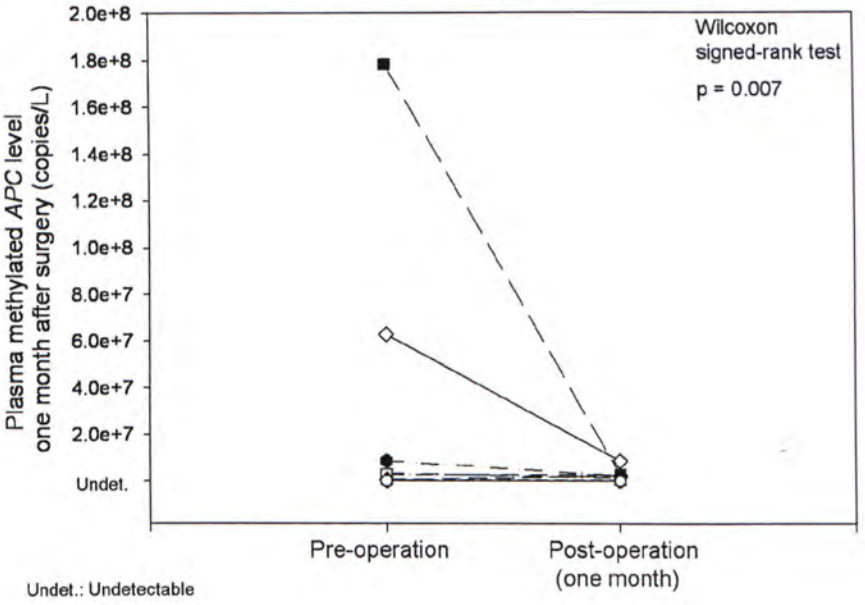

(D) *p16*

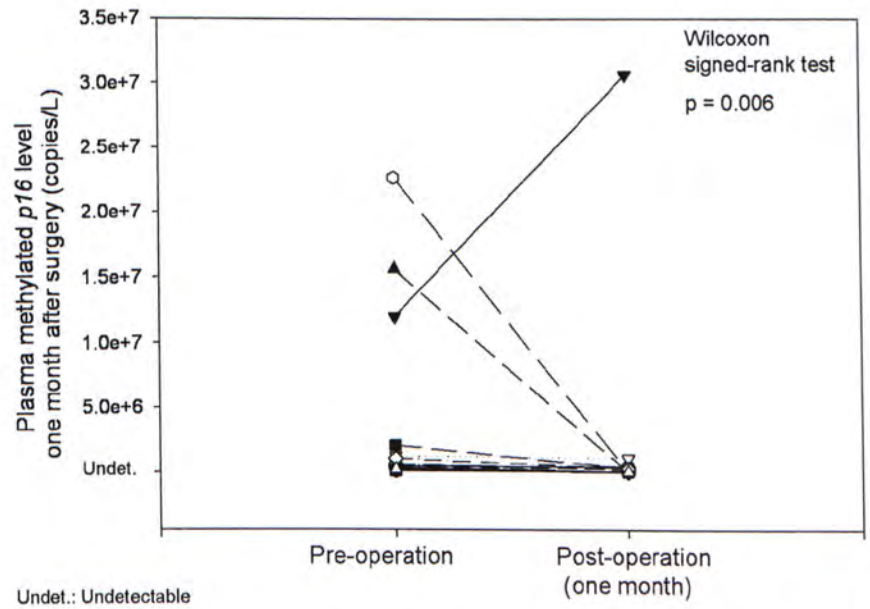

Figure 5.4.1. Reduction in the plasma levels of methylated *GSTP1 (A), SOCS1 (B), APC (C)* and *p16 (D)* sequences at one month after tumor resection for the 34 HCC patients

(y-axis indicates the concentrations of methylated TSGs sequences in copies/L)

5.5. Concurrent use of serum AFP level and plasma methylated markers for HCC diagnosis

Serum AFP level is clinically used to detect HCC and the commonly applied cut-off value is 20 μg/L. However, the sensitivity of AFP measurement for HCC is only around 60% (detailed discussion in Chapter 1). In this part, I would like to demonstrate the improvement of detection rate by the combination of AFP and methylated markers.

There were no correlation between the presence of at least one methylated markers and the serum AFP level ≥ 20 μg/L for either HCC patients (Chi-square test:, P = 0.857) or HBV carriers (Chi-square test, P = 0.525).

Using a cut-off value of 20 μg/L, 31 (55%) of the 56 HCC patients had an elevated AFP concentration and only 5 (9%) of the 55 HBV carriers had an elevated level. For the 45% of HCC patients with serum AFP concentration < 20 μg/L, 18 patients (72%) of them had at least one methylated marker in plasma. After combining the serum AFP level and the presence of methylated TSGs markers, the diagnostic sensitivity was increased to 87.5% (49 of 56) with a slight decrease of specificity to 78.2% (43 of 55).

The positive predictive value is the proportion of patients with positive test results who are correctly diagnosed. The negative predictive value is the proportion of patients with negative test results who are correctly diagnosed. Using the combination of AFP analyses and methylation marker, the positive predictive value

of the test is 96.2% and the negative predictive value is 86%.

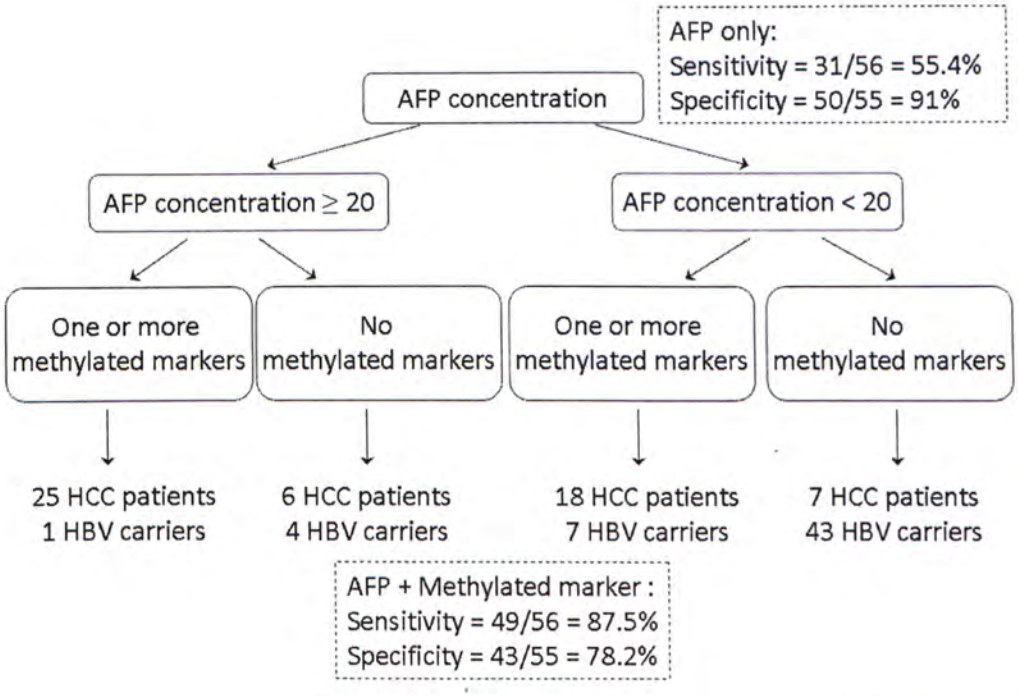

Figure 5.5.1. Classification of 56 patients and 55 HBV carriers according to their serum AFP concentrations and the presence of methylated TSG markers in their plasma

5.6. Prognostic value of plasma methylated TSGs

Kaplan-Meier survival curve is used to illustrate the survival probabilities of patients with detectable methylated *GSTP1*, *SOCS1*, *APC* and *p16* in plasma. Patients with and without detectable methylated *GSTP1*, *SOCS1*, *APC* and *p16* in plasma did not show significantly difference in disease-free survival probabilities (log-rank test, P = 0.43, 0.42, 0.73 and 0.15, respectively) (Figure 5.5.1). On the other hand, patients with two or more methylated markers in plasma at diagnosis had significantly poorer survival probability (log-rank test, P = 0.013) (Figure 5.5.2).

Cox proportional hazards regression analysis was performed to determine if the prognostic value of the number of markers is independent of other parameters (Table 5.5.1 and 5.5.2). The presence of two or more methylated markers in plasma at diagnosis was an independent predictor for disease free survival (Multivariate Cox proportional hazards regression, P = 0.039).

(I)

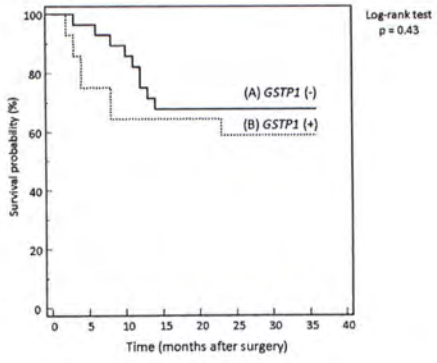

(II)

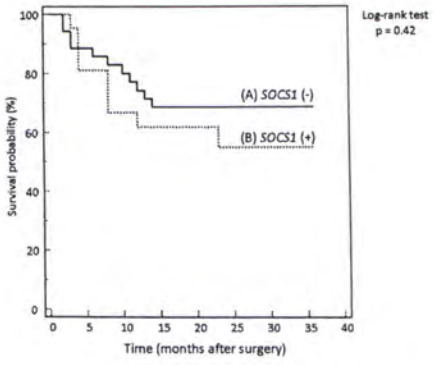

(III)

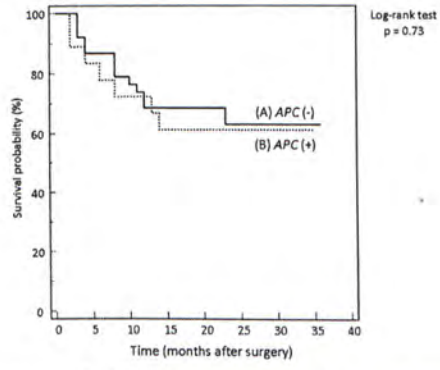

(IV)

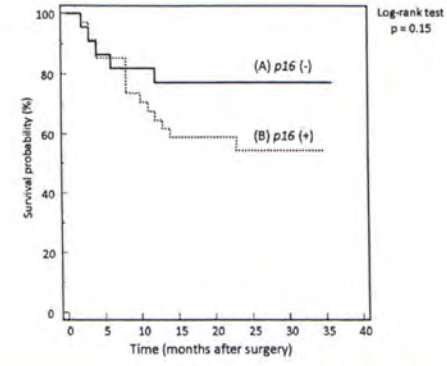

Figure 5.6.1. Recurrence-free survival curves for HCC patients. Patients with and without methylated (I) *GSTP1*, (II) *SOCS1*, (III) *APC*, (IV) *p16* in plasma at diagnosis

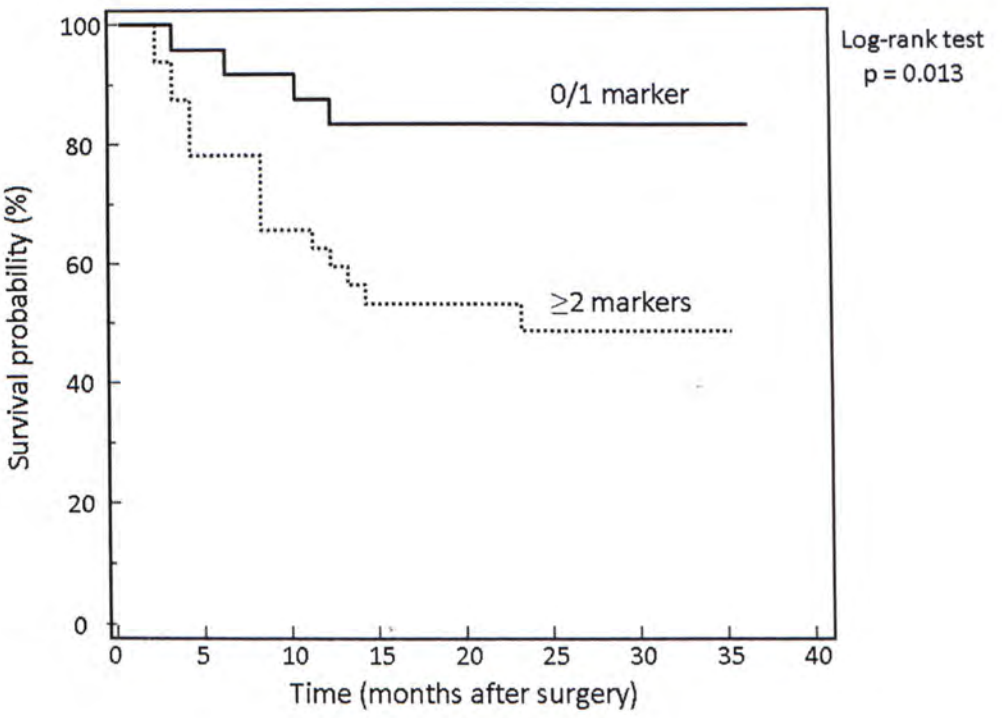

Figure 5.6.2. Recurrence-free survival curves for HCC patients

The Kaplan-Meier survival curve of patients with 2 or more methylated markers in plasma showed significantly poorer disease-free survival than those with 0 or 1 marker only at diagnosis.

Table 5.6.1. Univariate Cox-regression analysis of various factors on the recurrence-free survival in HCC patients

Covariate	P value	Hazard Ratio	95% confidence interval of hazard ratio
No. of markers: ≥2	**0.022**	**3.60**	**1.21-10.71**
Serum AFP: ≥20 μg/L	0.107	2.20	0.85-5.71
Cirrhosis	0.100	0.43	0.16-1.17
No. of lesions: >1	0.976	1.02	0.34-3.03
Size of tumor (in cm)	0.464	1.05	0.93-1.17
Detectable *GSTP1* level	0.438	1.42	0.59-3.41
Detectable *SOCS1* level	0.432	1.42	0.59-3.42
Detectable *APC* level	0.738	1.17	0.47-2.92
Detectable *p16* level	0.166	2.04	0.75-5.60

Table 5.6.2. Multivariate Cox-regression analysis of various factors on the recurrence-free survival in HCC patients

Covariate	P value	Hazard Ratio	95% confidence interval of hazard ratio
No. of markers: ≥2	**0.039**	**3.28**	**1.07-10.12**
Serum AFP: ≥20 μg/L	0.100	2.29	0.86-6.14
Cirrhosis	0.060	0.37	0.13-1.04
No.of lesions: >1	0.685	1.26	0.42-3.81
Size of tumor (in cm)	0.949	1.00	0.88-1.15

SECTION IV: DISCUSSION

Chapter 6: Discussion

HCC is a tumor of global public health problem. The surveillance of HCC still relies on the measurement of serum AFP level which has been used for 40 years. The discovery of hypermethylation of the promoters of tumor suppressor genes in HCC tissues has opened up the possibility of using methylated TSGs as potential markers for HCC. Technically, MSP has been a commonly used technique for the detection of aberrantly methylated TSGs in multiple biological specimens, including blood samples. However, the detection rates of methylated sequences in blood have been shown by previous work to be much lower than the detection rates in tumor tissues. It was likely the result of low concentrations of tumoral DNA in plasma/serum (Chan & Lo, 2007; Wong *et al*, 2003) and the degradation of DNA during the bisulfite conversion step of MSP (Grunau *et al*, 2001). In this regard, Chan *et al.* have developed a non-bisulfite-based approach to detect methylated *RASSF1A* in plasma. This method is based on the specific degradation of unmethylated sequence by methylation-sensitive restriction enzymes and the detection of undigestible methylated sequences by real-time PCR. They showed that this method is highly sensitive for detecting placental-derived methylated *RASSF1A* in maternal plasma (Chan *et al*, 2006a) and methylated tumoral *RASSF1A* sequences in the serum of HCC patients (Chan *et al*, 2008a). Using this method, hypermethylated *RASSF1A* sequences could be detected in the serum of 93% HCC patients. As the sensitivity was remarkably enhanced by this non-bisulfite approach, low concentrations of methylated *RASSF1A* sequences were also detected in the serum samples of 58% HBV carriers. This observation was postulated to be due to the release of methylated

sequences from the nonmalignant hepatitic liver as the hypermethylation of *RASSF1A* was an early event in HCC pathogenesis and could be observed in patients with nonmalignant conditions such as cirrhosis and chronic hepatitis (Chan *et al*, 2008a). In this project, I have studied the detectibility of other aberrantly methylated TSG in the plasma of HCC patients to determine if the combination of these markers can provide a more accurate diagnostic profile for HCC than using *RASSF1A* alone.

6.1. Tumor and plasma detection of hypermethylated tumor suppressor genes

The frequencies of hypermethylated *GSTP1, SOCS1, APC* and *p16* detected in tumor tissues using MSRE-qPCR were similar to previous studies using MSP which have been mentioned in Chapter 2.5.2. On the other hand, the detection rates of the tumor suppressor gene sequences in plasma were improved because the background unmethylated sequences were specifically degraded by the methylation-sensitive restriction enzymes. In contrast to the previous study on *RASSF1A*, the detection rates of hypermethylated *GSTP1, SOCS1, APC* and *p16* sequences in the plasma of HBV carriers were much lower. Hepatocarcinogenesis is a multistep process and promoter hypermethylation of *RASSF1A* involves in initial stage of HCC pathogenesis (Lee *et al*, 2003). Promoter hypermethylation of *GSTP1, SOCS1, APC* and *p16* genes may be a later event than that of *RASSF1A* and more specific to indicate the presence of a tumor.

The significant correlation between the plasma concentration of *p16* sequences with tumor size may reflect the tumor load that has also been suggested by other study (Chan *et al*, 2008a; Chan *et al*, 2005a). And the lack of correlation between other

tumor suppressor genes and tumor size may be related to the relatively lower proportion of the sequences in plasma with a high background of methylated sequences derived from nonmalignant hepatitis liver tissues.

In the current study, hypermethylation of *GSTP1* was detected in the tumor tissues of 78.6% HCC patients. Among the patients with *GSTP1* hypermethylated in tumor, methylated *GSTP1* sequences were detected in the plasma of 54.5% of them. This is translated to an overall detection rate of 42.9%. In contrast, only 3.6% HBV carriers and none of the healthy individuals had detectable methylated *GSTP1* sequences in plasma.

Hypermethylated *SOCS1* sequences were observed in 64.3% tumor tissues of HCC patients. Among these patients, methylated *SOCS1* sequences were detected in the plasma of 55.6% of them. This translates to an overall detection rate of 35.7% in HCC patients. In contrast, methylated *SOCS1* sequences were detected in the plasma of 3.6% in HBV carriers and 0% in healthy individuals.

Hypermethylated *APC* sequences were observed in 87.5% tumor tissues of HCC patients. Among these patients, methylated *APC* sequences were detected in the plasma of 36.7% of them. This translates to an overall detection rate of 32.1% in HCC patients. In contrast, methylated *APC* sequences were detected in the plasma of 0% in HBV carriers and 3.4% in healthy individuals.

Hypermethylated *p16* sequences were observed in 89.3% tumor tissues of HCC patients. Among these patients, methylated *p16* sequences were detected in the

plasma of 66% of them. This translates to an overall detection rate of 58.9% in HCC patients. In contrast, methylated *p16* sequences were detected in the plasma of 9.1% in HBV carriers and none of the healthy individuals.

Seventy-five percent of HCC tumor samples had the promoter of 3 or more methylated TSGs being hypermethylated while only one sample did not have any hypermethylation of any of the four TSGs. These results indicated that hypermethylation of TSGs is a prevalent event in HCC tissues and multiple signal transduction pathways are involved in the carcinogenesis of HCC. The detection rates of methylated sequence of these four TSGs range from 32.1 to 58.9%. In 76.8% of HCC patients, one or more methylated TSGs were detected in the plasma. In contrast, only 14.5% of the HBV carriers and 3.4 % of the healthy individuals had one or more methylated TSGs detectable in plasma. Therefore, the detection of methylated TSGs in plasma appears to be a useful diagnostic marker for HCC.

6.2. No effect of cirrhosis on plasma methylated DNA level

Hepatitis virus B/C infection and cirrhosis are the major etiological factors for HCC. Previous studies have demonstrated the hypermethylation of TSGs in the hepatic and cirrhotic livers (Kaneto *et al*, 2001; Kondo *et al*, 2000; Roncalli *et al*, 2002). However, in this project, I have shown that methylated TSG sequences are infrequently detected in the plasma of subjects with chronic HBV infection. Furthermore, the difference in the plasma levels of TSGs between HCC patients and HBV carriers is independent of the cirrhotic status of the subjects.

6.3. Clearance of methylated TSG sequences after tumor resection

To demonstrate the tumoral origin of the methylated TSG sequences in plasma, I have studied the changes in their concentrations after tumor resection. Above 80% of cases showed a reduction in the plasma concentration of methylated TSG sequences after surgical resection.

One particular case showed a sharp increase of 2.5 fold methylated *p16* sequences (from 1.2×10^7 copies/L to 3.1×10^7 copies/L) in plasma one month after surgery while the concentrations of the methylated *GSTP1* and *APC* sequences reduced from 7.5×10^6 copies/L to 2.3×10^6 copies/L and 8.4×10^6 copies/L to 2.3×10^6 copies/L respectively. No methylated *SOCS1* sequences were found in the preoperative and postoperative samples.This patient was HBV-associated, had cirrhosis, had a single 6 cm tumor and had an AFP value up to 20,000 μg/L. HCC recurred two months after surgery and the patient passed away six months after surgery.

For the observations concerning this sample, I postulated that in this patient the hypermethylation of the *p16* promoter would be the tumor specific change whereas the hypermethylation of the *GSTP1* and *APC* promoters might also be present in the background hepatitic and cirrhotic liver. The rapid rise in *p16* concentrations is in line with the rapid recurrence of the cancer and may indicate the increase in tumor load. On the other hand, the modest reduction in *GSTP1* and *APC* concentrations may represent the reduction of the liver size after hepatectomy.

6.4. Concurrent use of serum AFP level and the presence of methylated markers in the plasma in HCC diagnosis

I have shown in the previous chapter that the detection rate for HCC was 77% using the combination of the four TSGs with a specificity of 86%. On the other hand, AFP measurement gave a sensitivity of 55% and a specificity of 91%. The sensitivity of detecting HCC increased to 88% when they are used together and the specificity is 78%. Therefore, the combination of these two types of markers might improve the diagnostic accuracy of the existing surveillance program and improve the overall survival of HCC patients.

6.5. Prognostic significance of circulating methylated tumor markers

In addition to being useful for detecting HCC, these methylated markers are also of prognostic potential. It is interesting that the survival was not significantly correlated with the presence of any individual methylated TSGs at diagnosis. This finding is consistent with the observations in other previous studies on esophageal cancer (Brock *et al*, 2003; Hibi *et al*, 2001), lung cancer (Kim *et al*, 2005) and prostate cancer (Maruyama *et al*, 2002). In contrast, the presence of two or more methylated markers in plasma at diagnosis was associated with a poorer survival. There are several possible explanations for this observation. First, patients with more methylated markers in plasma may have a higher tumor load such that a higher and detectable concentrations of tumoral DNA are present in their plasma. Second, tumors may be more aggressive when more TSGs are methylated. Previous studies suggested that DNA methylation may accumulate as the molecular clock of a cancer advances with time (Brock *et al*, 2003).

The prognostic value of the number of TSG present in plasma was further shown to be not confounded by parameters including serum AFP level, cirrhosis, the size of

the tumor and the number of lesions in the liver (Multivariate Cox-regression analysis, P=0.04, HR=3.4).

SECTION V: CONCLUDING REMARKS

Chapter 7: Conclusions and future perspectives

Over the last decade, significant progress has been made to understand the molecular mechanisms involved in carcinogenesis. In this regard, hypermethylation of TSGs has been shown to be an important step in cancer formation, particularly in HCC where TSG mutations are uncommon. The advances in molecular biology have enabled the detection of such changes in blood or other body fluids and opens up new possibilities for non-invasive diagnosis of cancers. In this study, I have developed methylation-sensitive restriction enzymes-mediated quantitative PCR assays for the sensitive detection of aberrantly methylated TSGs including *GSTP1, SOCS1, APC* and *p16*. The reduction of methylated sequences in plasma at one month after tumor resection is highly suggestive for the tumoral origin of the circulating methylated DNA. With multiple tumor suppressor genes (*GSTP1, SOCS1, APC* and *p16*) combined in a panel, a detection rate of 76.8% can be achieved whereas only 14.5% in HBV carriers and 3.4% in healthy individuals had detectable TSGs in plasma. These methylated DNA markers can also be applied in conjunction with the existing HCC marker, AFP. This has improved the 55% sensitivity of AFP analysis to the 87.5% of using both markers.

Further improvement of detection accuracies by digital PCR

In this study, the experimental part was mostly dependent on the platform of real-time quantitative PCR which is inexpensive and can handle a moderate number of samples at a time. In fact, the detection sensitivity can still be improved if using another platform such as microfluidics digital PCR (Dube *et al*, 2008; Lun *et al*, 2008) that can generate more precise results. Digital PCR has been shown to be

superior to standard real-time PCR for detecting low concentration of targets (Yung *et al*, 2009). Digital MethyLight has been successfully used to detect hypermethylated sequences in plasma from breast cancer patients in a triplex manner (Weisenberger *et al*, 2008).

Routine clinical utility of methylated DNA markers

The measurement of serum AFP level is the most common blood test for HCC. However, it offers a sensitivity of only 40-60% and a specificity of 80-90% (Farinati *et al*, 2006; Wright *et al*, 2007). With the combination of multiple methylated DNA markers and serum AFP, a detection rate of 87.5% can be achieved with a slight decrease of specificity to 78.2% in HBV carriers. On the other hand, MSRE-qPCR is relatively inexpensive and technically simple. Therefore, the methylated DNA markers may be suitable for routine clinical practice for HCC diagnosis.

Diagnostic potential of methylated DNA markers for other cancers

Promoter hypermethylation of *GSTP1*, *SOCS1*, *APC* or *p16* are observed in many cancers. For example, methylated *GSTP1* sequences were detected in prostate cancer patients (Goessl *et al*, 2000) and methylated *APC* sequences were detected in oesophageal cancer patients (Kawakami *et al*, 2000). MSRE-qPCR assays developed in this study can be transferred to detect other cancers with hypermethylation of the *GSTP1*, *SOCS1*, *APC* or *p16* genes. MSRE-qPCR assays for other tumor suppressor genes can also be designed according to the methylation profiles of certain types of cancers.

Diagnostic potential of methylated DNA markers in other biological samples

MSRE-qPCR is sensitive in detecting methylated tumor suppressor genes sequences in plasma. The application of MSRE-qPCR may further be expanded to other body fluids such as urine and sputum samples. For instance, multiple methylated sequences have been detected in 90.9% urine sediment in bladder cancer using MSP (Chan *et al*, 2002). Therefore, with more sensitive MSRE-qPCR, the detection rate may be further improved.

The possibility of predicting the occurrence of HCC in healthy subjects or hepatitis carrier

Besides diagnostic utility, the methylated DNA markers may potentially be developed into predictive markers to predict the risk of an individual to develop HCC after certain period of time. Hypermethylation in promoter of tumor suppressor genes is an early event in carcinogenesis. It can be the first hit in Knudson's two-hit hypothesis. In many studies, methylated tumor suppressor genes sequences are also

detectable in premalignant tissue. Studies of the correlation between methylation statuses in premalignant tissues and the risk of developing HCC in the future are worthwhile. In this study, the methylation-sensitive restriction enzymes do not cut the DNA if the cytosines on both strands at the recognition sites are methylated, such that, the digestion is blocked by the methylated cytosines. Some methylation-sensitive restriction enzymes do not cut DNA with only one methylated cytosine at recognition sites. Assays can be further developed to detect the partially methylated statuses in DNA.

Further investigations on the diagnostic and prognostic potential of this panel of tumor markers are warranted as well as the clinical utility of the markers to predict chemotherapeutic response. The evaluation of the assays in high-throughput platform and large-scale studies are needed to further validate the results. In the near future, methylation markers have a great potential to develop into markers using in routine clinical diagnostics.

REFERENCES

Algar E. M., St Heaps L., Darmanian A., Dagar V., Prawitt D., Peters G. B., Collins F. (2007) Paternally inherited submicroscopic duplication at 11p15.5 implicates insulin-like growth factor II in overgrowth and Wilms' tumorigenesis. *Cancer Res* **67:** 2360-5

Azechi H., Nishida N., Fukuda Y., Nishimura T., Minata M., Katsuma H., Kuno M., Ito T., Komeda T., Kita R., Takahashi R., Nakao K. (2001) Disruption of the p16/cyclin D1/retinoblastoma protein pathway in the majority of human hepatocellular carcinomas. *Oncology* **60:** 346-54

Bird A. P. (1986) CpG-rich islands and the function of DNA methylation. *Nature* **321:** 209-13

Borzio M., Bruno S., Roncalli M., Mels G. C., Ramella G., Borzio F., Leandro G., Servida E., Podda M. (1995) Liver cell dysplasia is a major risk factor for hepatocellular carcinoma in cirrhosis: a prospective study. *Gastroenterology* **108:** 812-7

Bosch F. X., Ribes J., Diaz M., Cleries R. (2004) Primary liver cancer: worldwide incidence and trends. *Gastroenterology* **127:** S5-S16

Brock M. V., Gou M., Akiyama Y., Muller A., Wu T. T., Montgomery E., Deasel M., Germonpre P., Rubinson L., Heitmiller R. F., Yang S. C., Forastiere A. A., Baylin S. B., Herman J. G. (2003) Prognostic importance of promoter hypermethylation of multiple genes in esophageal adenocarcinoma. *Clin Cancer Res* **9:** 2912-9

But D. Y., Lai C. L., Yuen M. F. (2008) Natural history of hepatitis-related hepatocellular carcinoma. *World J Gastroenterol* **14:** 1652-6

Capurro M., Wanless I. R., Sherman M., Deboer G., Shi W., Miyoshi E., Filmus J. (2003) Glypican-3: a novel serum and histochemical marker for hepatocellular carcinoma. *Gastroenterology* **125:** 89-97

Chan H. L., Sung J. J. (2006) Hepatocellular carcinoma and hepatitis B virus. *Semin Liver Dis* **26:** 153-61

Chan K. C. A., Chan A. T., Leung S. F., Pang J. C., Wang A. Y., Tong J. H., To K. F., Chan L. Y., Tam L. L., Chung N. Y., Zhang J., Lo K. W., Huang D. P., Lo Y. M. D. (2005a) Investigation into the origin and tumoral mass correlation of plasma Epstein-Barr virus DNA in nasopharyngeal carcinoma. *Clin Chem* **51:** 2192-5

Chan K. C. A., Ding C., Gerovassili A., Yeung S. W., Chiu R. W. K., Leung T. N., Lau T. K., Chim S. S. C., Chung G. T., Nicolaides K. H., Lo Y. M. D. (2006a) Hypermethylated RASSF1A in maternal plasma: A universal fetal DNA marker that

improves the reliability of noninvasive prenatal diagnosis. *Clin Chem* **52:** 2211-8

Chan K. C. A., Lai P. B. S., Mok T. S., Chan H. L., Ding C., Yeung S. W., Lo Y. M. D. (2008a) Quantitative analysis of circulating methylated DNA as a biomarker for hepatocellular carcinoma. *Clin Chem* **54:** 1528-36

Chan K. C. A., Lo Y. M. D. (2006) Clinical applications of plasma Epstein-Barr virus DNA analysis and protocols for the quantitative analysis of the size of circulating Epstein-Barr virus DNA. *Methods Mol Biol* **336:** 111-21

Chan K. C. A., Lo Y. M. D. (2007) Circulating tumour-derived nucleic acids in cancer patients: potential applications as tumour markers. *Br J Cancer* **96:** 681-5

Chan Michael W. Y., Chan Lun W., Tang Nelson L. S., Tong Joanna H. M., Lo Kwok W., Lee Tin L., Cheung Ho Y., Wong Wai S., Chan Peter S. F., Lai Fernand M. M., To Ka F. (2002) Hypermethylation of Multiple Genes in Tumor Tissues and Voided Urine in Urinary Bladder Cancer Patients. *Clin Cancer Res* **8:** 464-470

Cheah M. S., Wallace C. D., Hoffman R. M. (1984) Hypomethylation of DNA in human cancer cells: a site-specific change in the c-myc oncogene. *J Natl Cancer Inst* **73:** 1057-65

Chiu R. W. K., Poon L. L., Lau T. K., Leung T. N., Wong E. M., Lo Y. M. D. (2001)

Effects of blood-processing protocols on fetal and total DNA quantification in maternal plasma. *Clin Chem* **47:** 1607-13

Costello J. F., Fruhwald M. C., Smiraglia D. J., Rush L. J., Robertson G. P., Gao X., Wright F. A., Feramisco J. D., Peltomaki P., Lang J. C., Schuller D. E., Yu L., Bloomfield C. D., Caligiuri M. A., Yates A., Nishikawa R., Su Huang H., Petrelli N. J., Zhang X., O'Dorisio M. S., Held W. A., Cavenee W. K., Plass C. (2000) Aberrant CpG-island methylation has non-random and tumour-type-specific patterns. *Nat Genet* **24:** 132-8

Csepregi A., Rocken C., Hoffmann J., Gu P., Saliger S., Muller O., Schneider-Stock R., Kutzner N., Roessner A., Malfertheiner P., Ebert M. P. (2008) APC promoter methylation and protein expression in hepatocellular carcinoma. *J Cancer Res Clin Oncol* **134:** 579-89

Dube S., Qin J., Ramakrishnan R. (2008) Mathematical analysis of copy number variation in a DNA sample using digital PCR on a nanofluidic device. *PLoS ONE* **3:** e2876

Dulaimi E., Hillinck J., Ibanez de Caceres I., Al-Saleem T., Cairns P. (2004) Tumor suppressor gene promoter hypermethylation in serum of breast cancer patients. *Clin Cancer Res* **10:** 6189-93

Eads C. A., Danenberg K. D., Kawakami K., Saltz L. B., Blake C., Shibata D., Danenberg P. V., Laird P. W. (2000) MethyLight: a high-throughput assay to measure DNA methylation. *Nucleic Acids Res* **28:** E32

El-Serag H. B. (2004) Hepatocellular carcinoma: recent trends in the United States. *Gastroenterology* **127:** S27-34

El-Serag H. B., Davila J. A., Petersen N. J., McGlynn K. A. (2003) The continuing increase in the incidence of hepatocellular carcinoma in the United States: an update. *Ann Intern Med* **139:** 817-23

Esteller M. (2008) Epigenetics in cancer. *N Engl J Med* **358:** 1148-59

Esteller M., Silva J. M., Dominguez G., Bonilla F., Matias-Guiu X., Lerma E., Bussaglia E., Prat J., Harkes I. C., Repasky E. A., Gabrielson E., Schutte M., Baylin S. B., Herman J. G. (2000a) Promoter hypermethylation and BRCA1 inactivation in sporadic breast and ovarian tumors. *J Natl Cancer Inst* **92:** 564-9

Esteller M., Sparks A., Toyota M., Sanchez-Cespedes M., Capella G., Peinado M. A., Gonzalez S., Tarafa G., Sidransky D., Meltzer S. J., Baylin S. B., Herman J. G. (2000b) Analysis of adenomatous polyposis coli promoter hypermethylation in human cancer. *Cancer Res* **60:** 4366-71

Farinati F., Marino D., De Giorgio M., Baldan A., Cantarini M., Cursaro C., Rapaccini G., Del Poggio P., Di Nolfo M. A., Benvegnu L., Zoli M., Borzio F., Bernardi M., Trevisani F. (2006) Diagnostic and prognostic role of alpha-fetoprotein in hepatocellular carcinoma: both or neither? *Am J Gastroenterol* **101:** 524-32

Feinberg A. P., Tycko B. (2004) The history of cancer epigenetics. *Nat Rev Cancer* **4:** 143-53

Frommer M., McDonald L. E., Millar D. S., Collis C. M., Watt F., Grigg G. W., Molloy P. L., Paul C. L. (1992) A genomic sequencing protocol that yields a positive display of 5-methylcytosine residues in individual DNA strands. *Proc Natl Acad Sci U S A* **89:** 1827-31

Gewirtz David A. (1999) A critical evaluation of the mechanisms of action proposed for the antitumor effects of the anthracycline antibiotics adriamycin and daunorubicin. *Biochemical Pharmacology* **57:** 727-741

Gibson U. E., Heid C. A., Williams P. M. (1996) A novel method for real time quantitative RT-PCR. *Genome Res* **6:** 995-1001

Glenn C. C., Deng G., Michaelis R. C., Tarleton J., Phelan M. C., Surh L., Yang T. P., Driscoll D. J. (2000) DNA methylation analysis with respect to prenatal diagnosis of the Angelman and Prader-Willi syndromes and imprinting. *Prenat Diagn* **20:** 300-6

Goessl C., Krause H., Muller M., Heicappell R., Schrader M., Sachsinger J., Miller K. (2000) Fluorescent methylation-specific polymerase chain reaction for DNA-based detection of prostate cancer in bodily fluids. *Cancer Res* **60:** 5941-5

Gonzalgo M. L., Jones P. A. (1997) Rapid quantitation of methylation differences at specific sites using methylation-sensitive single nucleotide primer extension (Ms-SNuPE). *Nucleic Acids Res* **25:** 2529-31

Grunau C., Clark S. J., Rosenthal A. (2001) Bisulfite genomic sequencing: systematic investigation of critical experimental parameters. *Nucleic Acids Res* **29:** E65-5

Hanash Samir M., Pitteri Sharon J., Faca Vitor M. (2008) Mining the plasma proteome for cancer biomarkers. *Nature* **452:** 571-579

Herman J. G., Baylin S. B. (2003) Gene silencing in cancer in association with promoter hypermethylation. *N Engl J Med* **349:** 2042-54

Herman J. G., Graff J. R., Myohanen S., Nelkin B. D., Baylin S. B. (1996) Methylation-specific PCR: a novel PCR assay for methylation status of CpG islands. *Proc Natl Acad Sci U S A* **93:** 9821-6

Herman J. G., Latif F., Weng Y., Lerman M. I., Zbar B., Liu S., Samid D., Duan D. S., Gnarra J. R., Linehan W. M., et al. (1994) Silencing of the VHL tumor-suppressor gene by DNA methylation in renal carcinoma. *Proc Natl Acad Sci U S A* **91:** 9700-4

Hibi K., Taguchi M., Nakayama H., Takase T., Kasai Y., Ito K., Akiyama S., Nakao A. (2001) Molecular detection of p16 promoter methylation in the serum of patients with esophageal squamous cell carcinoma. *Clin Cancer Res* **7:** 3135-8

Honda S., Haruta M., Sugawara W., Sasaki F., Ohira M., Matsunaga T., Yamaoka H., Horie H., Ohnuma N., Nakagawara A., Hiyama E., Todo S., Kaneko Y. (2008) The methylation status of RASSF1A promoter predicts responsiveness to chemotherapy and eventual cure in hepatoblastoma patients. *Int J Cancer* **123:** 1117-25

Hoque M. O., Feng Q., Toure P., Dem A., Critchlow C. W., Hawes S. E., Wood T., Jeronimo C., Rosenbaum E., Stern J., Yu M., Trink B., Kiviat N. B., Sidransky D. (2006) Detection of aberrant methylation of four genes in plasma DNA for the detection of breast cancer. *J Clin Oncol* **24:** 4262-9

Ikoma J., Kaito M., Ishihara T., Nakagawa N., Kamei A., Fujita N., Iwasa M., Tamaki S., Watanabe S., Adachi Y. (2002) Early diagnosis of hepatocellular carcinoma using a sensitive assay for serum des-gamma-carboxy prothrombin: a prospective study. *Hepatogastroenterology* **49:** 235-8

Jahr S., Hentze H., Englisch S., Hardt D., Fackelmayer F. O., Hesch R. D., Knippers R. (2001) DNA fragments in the blood plasma of cancer patients: quantitations and evidence for their origin from apoptotic and necrotic cells. *Cancer Res* **61:** 1659-65

Jones P. A., Baylin S. B. (2002) The fundamental role of epigenetic events in cancer. *Nat Rev Genet* **3:** 415-28

Kaneto H., Sasaki S., Yamamoto H., Itoh F., Toyota M., Suzuki H., Ozeki I., Iwata N., Ohmura T., Satoh T., Karino Y., Toyota J., Satoh M., Endo T., Omata M., Imai K. (2001) Detection of hypermethylation of the p16(INK4A) gene promoter in chronic hepatitis and cirrhosis associated with hepatitis B or C virus. *Gut* **48:** 372-7

Katoh H., Shibata T., Kokubu A., Ojima H., Fukayama M., Kanai Y., Hirohashi S. (2006) Epigenetic instability and chromosomal instability in hepatocellular carcinoma. *Am J Pathol* **168:** 1375-84

Kawakami K., Brabender J., Lord R. V., Groshen S., Greenwald B. D., Krasna M. J., Yin J., Fleisher A. S., Abraham J. M., Beer D. G., Sidransky D., Huss H. T., Demeester T. R., Eads C., Laird P. W., Ilson D. H., Kelsen D. P., Harpole D., Moore M. B., Danenberg K. D., Danenberg P. V., Meltzer S. J. (2000) Hypermethylated APC DNA in plasma and prognosis of patients with esophageal adenocarcinoma. *J Natl Cancer Inst* **92:** 1805-11

Kim Y. T., Park S. J., Lee S. H., Kang H. J., Hahn S., Kang C. H., Sung S. W., Kim J. H. (2005) Prognostic implication of aberrant promoter hypermethylation of CpG islands in adenocarcinoma of the lung. *J Thorac Cardiovasc Surg* **130:** 1378

Knudson A. G. (2001) Two genetic hits (more or less) to cancer. *Nat Rev Cancer* **1:** 157-62

Kondo Y., Kanai Y., Sakamoto M., Mizokami M., Ueda R., Hirohashi S. (2000) Genetic instability and aberrant DNA methylation in chronic hepatitis and cirrhosis--A comprehensive study of loss of heterozygosity and microsatellite instability at 39 loci and DNA hypermethylation on 8 CpG islands in microdissected specimens from patients with hepatocellular carcinoma. *Hepatology* **32:** 970-9

Laird P. W. (2003) The power and the promise of DNA methylation markers. *Nat Rev Cancer* **3:** 253-66

Lau W. Y. (2008) *Hepatocellular carcinoma*. Hackensack, NJ: World Scientific Pub.

Lee S., Lee H. J., Kim J. H., Lee H. S., Jang J. J., Kang G. H. (2003) Aberrant CpG island hypermethylation along multistep hepatocarcinogenesis. *Am J Pathol* **163:** 1371-8

Lee W. H., Morton R. A., Epstein J. I., Brooks J. D., Campbell P. A., Bova G. S., Hsieh W. S., Isaacs W. B., Nelson W. G. (1994) Cytidine methylation of regulatory sequences near the pi-class glutathione S-transferase gene accompanies human prostatic carcinogenesis. *Proc Natl Acad Sci U S A* **91:** 11733-7

Livraghi Tito, Makuuchi Masatoshi, Buscarini Luigi (1997) *Diagnosis and treatment of hepatocellular carcinoma*. London: Greenwich Medical Media

Llovet J. M., Bruix J. (2003) Systematic review of randomized trials for unresectable hepatocellular carcinoma: Chemoembolization improves survival. *Hepatology* **37:** 429-42

Llovet J. M., Burroughs A., Bruix J. (2003) Hepatocellular carcinoma. *Lancet* **362:** 1907-17

Llovet J. M., Fuster J., Bruix J. (1999) Intention-to-treat analysis of surgical treatment for early hepatocellular carcinoma: resection versus transplantation. *Hepatology* **30:** 1434-40

Lo Y. M. D., Wong I. H. N., Zhang J., Tein M. S., Ng M. H., Hjelm N. M. (1999) Quantitative analysis of aberrant p16 methylation using real-time quantitative methylation-specific polymerase chain reaction. *Cancer Res* **59:** 3899-903

Lun F. M., Chiu R. W., Allen Chan K. C., Yeung Leung T., Kin Lau T., Dennis Lo Y. M. (2008) Microfluidics digital PCR reveals a higher than expected fraction of fetal DNA in maternal plasma. *Clin Chem* **54:** 1664-72

Maeta Y., Shiota G., Okano J., Murawaki Y. (2005) Effect of promoter methylation of the p16 gene on phosphorylation of retinoblastoma gene product and growth of hepatocellular carcinoma cells. *Tumour Biol* **26:** 300-5

Mannervik B., Alin P., Guthenberg C., Jensson H., Tahir M. K., Warholm M., Jornvall H. (1985) Identification of three classes of cytosolic glutathione transferase common to several mammalian species: correlation between structural data and enzymatic properties. *Proc Natl Acad Sci U S A* **82:** 7202-6

Marrero J. A., Romano P. R., Nikolaeva O., Steel L., Mehta A., Fimmel C. J., Comunale M. A., D'Amelio A., Lok A. S., Block T. M. (2005) GP73, a resident Golgi glycoprotein, is a novel serum marker for hepatocellular carcinoma. *J Hepatol* **43:** 1007-12

Marrero Jorge A., Lok Anna S. F. (2004) Newer markers for hepatocellular carcinoma. *Gastroenterology* **127:** S113-S119

Maruyama R., Toyooka S., Toyooka K. O., Virmani A. K., Zochbauer-Muller S., Farinas A. J., Minna J. D., McConnell J., Frenkel E. P., Gazdar A. F. (2002) Aberrant

promoter methylation profile of prostate cancers and its relationship to clinicopathological features. *Clin Cancer Res* **8:** 514-9

McClelland M. (1981) The effect of sequence specific DNA methylation on restriction endonuclease cleavage. *Nucleic Acids Res* **9:** 5859-66

Merlo A., Herman J. G., Mao L., Lee D. J., Gabrielson E., Burger P. C., Baylin S. B., Sidransky D. (1995) 5' CpG island methylation is associated with transcriptional silencing of the tumour suppressor p16/CDKN2/MTS1 in human cancers. *Nat Med* **1:** 686-92

Michielsen P. P., Francque S. M., van Dongen J. L. (2005) Viral hepatitis and hepatocellular carcinoma. *World J Surg Oncol* **3:** 27

Miura N., Maeda Y., Kanbe T., Yazama H., Takeda Y., Sato R., Tsukamoto T., Sato E., Marumoto A., Harada T., Sano A., Kishimoto Y., Hirooka Y., Murawaki Y., Hasegawa J., Shiota G. (2005) Serum human telomerase reverse transcriptase messenger RNA as a novel tumor marker for hepatocellular carcinoma. *Clin Cancer Res* **11:** 3205-9

Miyoshi H., Fujie H., Moriya K., Shintani Y., Tsutsumi T., Makuuchi M., Kimura S., Koike K. (2004) Methylation status of suppressor of cytokine signaling-1 gene in hepatocellular carcinoma. *J Gastroenterol* **39:** 563-9

Morgan T. R., Mandayam S., Jamal M. M. (2004) Alcohol and hepatocellular carcinoma. *Gastroenterology* **127:** S87-96

Nagai H., Kim Y. S., Konishi N., Baba M., Kubota T., Yoshimura A., Emi M. (2002) Combined hypermethylation and chromosome loss associated with inactivation of SSI-1/SOCS-1/JAB gene in human hepatocellular carcinomas. *Cancer Lett* **186:** 59-65

Nishida N., Nagasaka T., Nishimura T., Ikai I., Boland C. R., Goel A. (2008) Aberrant methylation of multiple tumor suppressor genes in aging liver, chronic hepatitis, and hepatocellular carcinoma. *Hepatology* **47:** 908-18

Nishida N., Nishimura T., Nagasaka T., Ikai I., Goel A., Boland C. R. (2007) Extensive methylation is associated with beta-catenin mutations in hepatocellular carcinoma: evidence for two distinct pathways of human hepatocarcinogenesis. *Cancer Res* **67:** 4586-94

Oka H., Saito A., Ito K., Kumada T., Satomura S., Kasugai H., Osaki Y., Seki T., Kudo M., Tanaka M. (2001) Multicenter prospective analysis of newly diagnosed hepatocellular carcinoma with respect to the percentage of Lens culinaris agglutinin-reactive alpha-fetoprotein. *J Gastroenterol Hepatol* **16:** 1378-83

Okano M., Bell D. W., Haber D. A., Li E. (1999) DNA methyltransferases Dnmt3a and Dnmt3b are essential for de novo methylation and mammalian development. *Cell* **99:** 247-57

Okano M., Xie S., Li E. (1998) Cloning and characterization of a family of novel mammalian DNA (cytosine-5) methyltransferases. *Nat Genet* **19:** 219-20

Okochi O., Hibi K., Sakai M., Inoue S., Takeda S., Kaneko T., Nakao A. (2003) Methylation-mediated silencing of SOCS-1 gene in hepatocellular carcinoma derived from cirrhosis. *Clin Cancer Res* **9:** 5295-8

Okuda K. (1992) Hepatocellular carcinoma: recent progress. *Hepatology* **15:** 948-63

Parkin D. M., Bray F., Ferlay J., Pisani P. (2005) Global cancer statistics, 2002. *CA Cancer J Clin* **55:** 74-108

Paulsen M., Ferguson-Smith A. C. (2001) DNA methylation in genomic imprinting, development, and disease. *J Pathol* **195:** 97-110

Poon T. C., Mok T. S., Chan A. T., Chan C. M., Leong V., Tsui S. H., Leung T. W., Wong H. T., Ho S. K., Johnson P. J. (2002) Quantification and utility of monosialylated alpha-fetoprotein in the diagnosis of hepatocellular carcinoma with nondiagnostic serum total alpha-fetoprotein. *Clin Chem* **48:** 1021-7

Pradhan S., Bacolla A., Wells R. D., Roberts R. J. (1999) Recombinant human DNA (cytosine-5) methyltransferase. I. Expression, purification, and comparison of de novo and maintenance methylation. *J Biol Chem* **274:** 33002-10

Rapaccini G. L., Pompili M., Caturelli E., Covino M., Lippi M. E., Beccaria S., Cedrone A., Riccardi L., Siena D. A., Gasbarrini G. (2004) Hepatocellular carcinomas <2 cm in diameter complicating cirrhosis: ultrasound and clinical features in 153 consecutive patients. *Liver Int* **24:** 124-30

Reik W., Ferguson-Smith A. C. (2005) Developmental biology: the X-inactivation yo-yo. *Nature* **438:** 297-8

Roncalli M., Bianchi P., Bruni B., Laghi L., Destro A., Di Gioia S., Gennari L., Tommasini M., Malesci A., Coggi G. (2002) Methylation framework of cell cycle gene inhibitors in cirrhosis and associated hepatocellular carcinoma. *Hepatology* **36:** 427-32

Sangiovanni A., Del Ninno E., Fasani P., De Fazio C., Ronchi G., Romeo R., Morabito A., De Franchis R., Colombo M. (2004) Increased survival of cirrhotic patients with a hepatocellular carcinoma detected during surveillance. *Gastroenterology* **126:** 1005-14

Smela M. E., Currier S. S., Bailey E. A., Essigmann J. M. (2001) The chemistry and biology of aflatoxin B(1): from mutational spectrometry to carcinogenesis. *Carcinogenesis* **22:** 535-45

Song B. C., Chung Y. H., Kim J. A., Choi W. B., Suh D. D., Pyo S. I., Shin J. W., Lee H. C., Lee Y. S., Suh D. J. (2002) Transforming growth factor-beta1 as a useful serologic marker of small hepatocellular carcinoma. *Cancer* **94:** 175-80

Starr R., Willson T. A., Viney E. M., Murray L. J., Rayner J. R., Jenkins B. J., Gonda T. J., Alexander W. S., Metcalf D., Nicola N. A., Hilton D. J. (1997) A family of cytokine-inducible inhibitors of signalling. *Nature* **387:** 917-21

Straub T., Becker P. B. (2007) Dosage compensation: the beginning and end of generalization. *Nat Rev Genet* **8:** 47-57

Su P. F., Lee T. C., Lin P. J., Lee P. H., Jeng Y. M., Chen C. H., Liang J. D., Chiou L. L., Huang G. T., Lee H. S. (2007) Differential DNA methylation associated with hepatitis B virus infection in hepatocellular carcinoma. *Int J Cancer* **121:** 1257-64

Suzuki M., Shiraha H., Fujikawa T., Takaoka N., Ueda N., Nakanishi Y., Koike K., Takaki A., Shiratori Y. (2005) Des-gamma-carboxy prothrombin is a potential autologous growth factor for hepatocellular carcinoma. *J Biol Chem* **280:** 6409-15

Tangkijvanich P., Tosukhowong P., Bunyongyod P., Lertmaharit S., Hanvivatvong O., Kullavanijaya P., Poovorawan Y. (1999) Alpha-L-fucosidase as a serum marker of hepatocellular carcinoma in Thailand. *Southeast Asian J Trop Med Public Health* **30:** 110-4

Tollefsbol Trygve O. (2009) *Cancer epigenetics*. Boca Raton: CRC Press

Tsai J. F., Jeng J. E., Chuang L. Y., You H. L., Ho M. S., Lai C. S., Wang L. Y., Hsieh M. Y., Chen S. C., Chuang W. L., Lin Z. Y., Yu M. L., Dai C. Y. (2003) Serum insulin-like growth factor-II and alpha-fetoprotein as tumor markers of hepatocellular carcinoma. *Tumour Biol* **24:** 291-8

Tsukuma H., Hiyama T., Tanaka S., Nakao M., Yabuuchi T., Kitamura T., Nakanishi K., Fujimoto I., Inoue A., Yamazaki H., et al. (1993) Risk factors for hepatocellular carcinoma among patients with chronic liver disease. *N Engl J Med* **328:** 1797-801

Umemura T., Ichijo T., Yoshizawa K., Tanaka E., Kiyosawa K. (2009) Epidemiology of hepatocellular carcinoma in Japan. *J Gastroenterol* **44 Suppl 19:** 102-7

Vachtenheim J., Horakova I., Novotna H. (1994) Hypomethylation of CCGG sites in the 3' region of H-ras protooncogene is frequent and is associated with H-ras allele loss in non-small cell lung cancer. *Cancer Res* **54:** 1145-8

Wang J., Qin Y., Li B., Sun Z., Yang B. (2006) Detection of aberrant promoter methylation of GSTP1 in the tumor and serum of Chinese human primary hepatocellular carcinoma patients. *Clin Biochem* **39:** 344-8

Weisenberger D. J., Trinh B. N., Campan M., Sharma S., Long T. I., Ananthnarayan S., Liang G., Esteva F. J., Hortobagyi G. N., McCormick F., Jones P. A., Laird P. W. (2008) DNA methylation analysis by digital bisulfite genomic sequencing and digital MethyLight. *Nucleic Acids Res* **36:** 4689-98

Weksberg R., Shuman C., Smith A. C. (2005) Beckwith-Wiedemann syndrome. *Am J Med Genet C Semin Med Genet* **137C:** 12-23

Wong I. H. N., Lo Y. M. D., Zhang J., Liew C. T., Ng M. H., Wong N., Lai P. B. S., Lau W. Y., Hjelm N. M., Johnson P. J. (1999) Detection of aberrant p16 methylation in the plasma and serum of liver cancer patients. *Cancer Res* **59:** 71-3

Wong I. H. N., Yeo W., Leung T., Lau W. Y., Johnson P. J. (2001) Circulating tumor cell mRNAs in peripheral blood from hepatocellular carcinoma patients under radiotherapy, surgical resection or chemotherapy: a quantitative evaluation. *Cancer Lett* **167:** 183-91

Wong I. H. N., Zhang J., Lai P. B. S., Lau W. Y., Lo Y. M. D. (2003) Quantitative analysis of tumor-derived methylated p16INK4a sequences in plasma, serum, and

blood cells of hepatocellular carcinoma patients. *Clin Cancer Res* **9:** 1047-52

Wood A. J., Oakey R. J. (2006) Genomic imprinting in mammals: emerging themes and established theories. *PLoS Genet* **2:** e147

Wright Lorinda M., Kreikemeier Jeff T., Fimmel Claus J. (2007) A concise review of serum markers for hepatocellular cancer. *Cancer Detection and Prevention* **31:** 35-44

Xiong Z., Laird P. W. (1997) COBRA: a sensitive and quantitative DNA methylation assay. *Nucleic Acids Res* **25:** 2532-4

Yang B., Guo M., Herman J. G., Clark D. P. (2003) Aberrant promoter methylation profiles of tumor suppressor genes in hepatocellular carcinoma. *Am J Pathol* **163:** 1101-7

Yeo W., Wong N., Wong W. L., Lai P. B. S., Zhong S., Johnson P. J. (2005) High frequency of promoter hypermethylation of RASSF1A in tumor and plasma of patients with hepatocellular carcinoma. *Liver Int* **25:** 266-72

Yoshikawa H., Matsubara K., Qian G. S., Jackson P., Groopman J. D., Manning J. E., Harris C. C., Herman J. G. (2001) SOCS-1, a negative regulator of the JAK/STAT pathway, is silenced by methylation in human hepatocellular carcinoma and shows

growth-suppression activity. *Nat Genet* **28:** 29-35

Yung T. K., Chan K. C. A., Mok T. S., Tong J., To K. F., Lo Y. M. D. (2009) Single-molecule detection of epidermal growth factor receptor mutations in plasma by microfluidics digital PCR in non-small cell lung cancer patients. *Clin Cancer Res* **15:** 2076-84

Zhang Y. J., Chen Y., Ahsan H., Lunn R. M., Chen S. Y., Lee P. H., Chen C. J., Santella R. M. (2005) Silencing of glutathione S-transferase P1 by promoter hypermethylation and its relationship to environmental chemical carcinogens in hepatocellular carcinoma. *Cancer Lett* **221:** 135-43

Zhang Y. J., Wu H. C., Shen J., Ahsan H., Tsai W. Y., Yang H. I., Wang L. Y., Chen S. Y., Chen C. J., Santella R. M. (2007) Predicting hepatocellular carcinoma by detection of aberrant promoter methylation in serum DNA. *Clin Cancer Res* **13:** 2378-84

Zhong S., Tang M. W., Yeo W., Liu C., Lo Y. M. D., Johnson P. J. (2002) Silencing of GSTP1 gene by CpG island DNA hypermethylation in HBV-associated hepatocellular carcinomas. *Clin Cancer Res* **8:** 1087-92

Zhong S., Yeo W., Tang M. W., Wong N., Lai P. B. S., Johnson P. J. (2003) Intensive hypermethylation of the CpG island of Ras association domain family 1A in

hepatitis B virus-associated hepatocellular carcinomas. *Clin Cancer Res* **9:** 3376-82

Zhou L., Liu J., Luo F. (2006) Serum tumor markers for detection of hepatocellular carcinoma. *World J Gastroenterol* **12:** 1175-81